UNIVERSITY OF CALIFORNIA

Radiation Laboratory

BERKELEY, CALIFORNIA

DISCLAIMER

UCRL 703

Photo-Mesons from Carbon

by

Jack Milton Peterson
B.S. (Harvard University) 1942

DISSERTATION

Submitted in partial satisfaction of the requirements for the degree of

DOCTOR OF PHILOSOPHY

in

Physics

in the

GRADUATE DIVISION

of the

UNIVERSITY OF CALIFORNIA

Approved:

. . . . . .

. . . . . .

. . . . . .

. . . . . .

Committee in Charge

Deposited in the University Library . . . . . .
Date Librarian

TABLE OF CONTENTS

I. INTRODUCTION

History and Background

The production of mesons by photons was established for the first time when observed in the x-ray beam of the 322 Mev electron synchrotron at the University of California Radiation Laboratory by McMillan and Peterson[1] in January 1949. Photomesons occur also in high energy cosmic ray electron-photon showers but are easily obscured by the large number of other simultaneous events. They were reported observed in such showers for the first time later in 1949 by Fretter and Ise.[2]

It seems likely that the study of mesons produced in photon-nucleon interactions will be of greater value to meson theory than the study of those produced in nucleon-nucleon interactions, although the latter have available in the laboratory for a longer period. The main virtue of the photon-nucleon interaction, as has been pointed out by Brueckner,[3] is that the theoretical analysis of results is simplified by the nature of the interaction.

The ideal targets to bombard with photons are either protons or neutrons. Ordinary hydrogen is perfect for the former, and deuterium is the nearest experimental approach to the latter. Experiments using hydrogen and deuterium targets are now in progress.

The first pure target material bombarded by the x-ray beam was carbon. Carbon was chosen because of its relatively low atomic number and its ready availability and ease of fabrication. The background of such an experiment is due largely to electrons, positrons, and photons produced and scattered in the target material which tend to fog the nuclear emulsions used as detectors in this experiment. Since the pair production cross section varies

as the second power of the atomic number while meson production varies by no more than the first power, one improves the signal to background ratio by going to as low an atomic number as possible.

Although it was realized that with a carbon target one might not get a true picture of a pure photon-nucleon interaction because of possible distortion by the other nucleons in a carbon nucleus, it was felt that one might get a first approximation. Also if distortion by neighboring nucleons is important, it could be measured by comparison of the negative and positive meson spectra from carbon with those from hydrogen and deuterium. Furthermore, the energy spectrum and the ratio of negative to positive mesons from carbon are each of interest per se.

An earlier exploratory experiment[3] using a line target of carbon had given a rough energy spectrum of mesons emitted near 90° to the beam direction in the laboratory system. It had indicated that the angular distribution of mesons was approximately spherically symmetric, at least in the region near 90°, and also that more negative π-mesons are produced than positive by a ratio of 1.7 ± 0.2. The present experiment was designed to display more fully the angular and energy spectrum of mesons produced in carbon by x-rays generated by 322 Mev electrons.

II. EXPERIMENTAL METHOD

A. Experimental Procedure

The x-rays are produced in the Berkeley synchrotron by letting the 322 (± 5) Mev electron beam strike a 0.020 inch platinum target placed on the inner side of the accelerating tube. (See Figure 1.) The resultant x-ray beam emerges from the machine in a narrow cone whose full width at half intensity is 0.0135 radian (0.77 degree). At 55 inches from the platinum target the beam is collimated by a tapered hole in a lead block six inches thick. The collimating hole is 0.50 inch in diameter at the entrance end and is part of a cone whose apex is at the platinum target. This primary collimator defines by geometry a cone of x-rays whose full width is 0.0091 radian (0.52 degree). Directly behind the primary collimator is the secondary collimator, a three inch thickness of lead in which there is a cylindrical hole just slightly larger than the geometrically defined beam. The purpose of this seccndary collimator is to shield the detection equipment from the spray of electrons, positrons, and secondary photons produced in the walls of the primary collimator.

The x-ray beam strikes the spherical carbon target 4.5 inches from the exit of the secondary collimator. The diameter of the carbon sphere is 0.620 inch, just equal to the diameter of the diverging x-ray beam at that point. That the beam size was accurately determined by the geometry was confirmed by photographic film measurements.

The carbon target is surrounded by a large cylinder of copper, in which are imbedded stacks of nuclear emulsion plates. (See Figures 2, 3, and 4.) Mesons emitted from the carbon are slowed down and stopped throughout a large volume of the copper, and the imbedded emulsions serve to sample the meson density at various points. Both the energies and angles of the

emitted mesons can be determined by the positions of the meson endings--to within uncertainties due to scattering and to the finite size of the target.

The intensity of the x-ray beam is practically constant as it traverses the carbon target. The part of the beam which traverses the thickest region of the carbon is attenuated only 3.5 percent. Some fifteen feet beyond the carbon target the x-ray beam strikes a large ionization chamber which serves as the monitor in this experiment.

B. Experimental Design

The above description lists the main features of the experiment. Let us now discuss in more detail some of the considerations which went into the design of the components.

1. Use of nuclear emulsions. At the start of the experiment the nuclear emulsion technique was the only one that had been successfully used for the detection of photomesons. Since then Steinberger et al.[4] have developed a reliable electronic technique for the detection of positive π-mesons. The electronic techniques invariably have higher counting rates than those of the emulsion method, but the emulsion method is still the only one which can reliably detect negative π-mesons as well as positive. Furthermore, the emulsion method allows one to collect at no extra cost other interesting data, such as, for example, the energy and angular distributions of positive μ-mesons. The Ilford type C-2 emulsion was chosen because its sensitivity was felt to be optimum for the recognition of meson endings and yet great enough to allow easy recognition of relatively faint μ-tracks at the end of positive π-tracks. In a C-2 emulsion of normal background one can follow meson tracks of energies of up to about 12 Mev and proton tracks of energies up to 75 Mev or more. Electrons passing through this emulsion will leave

developable grains at only a relatively few points along its path--so few that an electron track cannot normally be recognized. These grains form a single-grain background in the emulsions and were the determining factor in the amount of exposure which could be used in this experiment. The emulsions used were nominally 100 microns in thickness.

2. Absorber medium. Since the meson density drops off as the inverse square of the distance from the carbon target, a relatively dense material such as copper or lead was desirable as the absorbing material. The stopping power of a unit thickness of copper is a few percent greater than that of lead. The bigger advantage of copper, however, is that the multiple Coulomb scattering per unit stopping power is only about half that of lead. The rms angle of multiple scatter from the carbon target to the point where a meson is first detected in the emulsion can be up to 47° for a lead absorber and up to 26° for copper. Since most of the scattering takes place in the last part of the meson's trajectory, which usually is in glass, the rms angle of scatter for a typical meson is 24° for a lead absorber and 18° for copper. The angle of emission of the meson, however, is determined not by its apparent angle when it enters the emulsion but rather by its position relative to the carbon target.

Since the scattering in the copper absorber is fairly large, it was decided to use completely poor geometry in the meson detection system. Thus the copper absorber was made in the form of a large cylinder surrounding the carbon target, as shown in Figures 2, 3, and 4. From the symmetry of the system it is seen that for every meson scattered out of a geometrical ray from the carbon source, there will be another scattered in, so that there is no net loss of meson density due to scattering. This statement contains implicitly the assumption that the angular distribution is a slowly varying

function of angular position. Throughout the experiment we treat the distribution in ϕ (the azimuthal angle about the x-ray beam axis) as constant because the x-ray beam is unpolarized. The scattering in the absorber will of course help to obscure any possible fine structure whose characteristic width in θ (the polar angle measured with respect to the forward direction of the x-ray beam axis) is less than about $\pm 7^{\circ}$, the total angular uncertainty of this experiment.

As indicated in Figures 2 and 3 there are 14 slots in the outer edge of the copper cylinder cut radial to the x-ray beam axis. In these slots are copper boxes containing stacks of nuclear plates. Each box had inside dimensions of about 7/8 in. x 1 in. x 9 in. Since the dimension of each plate is about 1/16 in. x 1 in. x 3 in., each box had space for 3 stacks of plates placed end to end, each stack containing about 14 plates. The plates were oriented so that the planes of the emulsions were approximately radial. There were 3 reasons for using this fairly large stack of plates at each position: (a) in order to determine the energy of the meson with any accuracy it is necessary to prevent the detection of mesons which enter the stack through the side rather than through the front, which faces toward the carbon target. By making the stack fourteen plates thick and using only the central six plates as detectors, one makes the detection of side-entering mesons unlikely; (b) the removal of a portion of the detectors at several times during a run allows one a variety of exposures under well controlled conditions and is economical with respect to synchrotron operating time; and (c) the possession of duplicate plates for each exposure is worthwhile protection against loss by breakage.

The difference in copper absorber thickness between consecutive plate positionswas 1/3 inch. Since the stopping power of an inch of the glass

used was just slightly greater than 1/3 inch of copper, this allowed the whole meson energy spectrum to be observed, excepting, of course, those energies below a minimum energy determined by self-absorption in the carbon target. The keyhole slot at the bottom of the copper cylinder extended into the 2 inch diameter cylindrical hole through which the x-ray beam passed. The copper box in this slot was open (except for two layers of Scotch photographic tape) on the side toward the carbon target and detected the lowest energy group of mesons. It is shown in Figures 2 and 4.

3. Shape and size of carbon target. The spherical shape of the target was chosen as an approximation to a point source of mesons so as to afford sufficient angular resolution in the detection of the mesons. If a line source had been used one would have had to use the angle at which the detected mesons entered the emulsion. As was noted in the previous section, the scattering in the absorbing materials makes this angle unreliable. Also, of course, the spherical shape allows the source to have the same appearance and characteristics in all directions of observation.

The size of the carbon target was determined by the minimum detectable meson energy which was compatible with a reasonable exposure time. The minimum energy detected was taken as the energy of a meson which is just able to traverse 0.75 of the radius of the carbon sphere, the mean thickness traversed by all mesons leaving the target. Since the minimum energy detected varies as roughly the square root of the target radius whereas the meson density, or exposure time for a given meson density, varies as the cube of the radius, it is apparent that it becomes increasingly difficult as one goes to very low minimum energies. With the target size used, the minimum energy was 12.5 Mev and the exposure time was 16 hours. To have reduced the target until the minimum energy was about 6 Mev would have required an exposure about 64 times as

long to get the same meson density. These figures are, moreover, unduly optimistic because we have assumed that the background is proportional to the target size. Actually with the target used a substantial part of the background was due to electron-positron pairs and secondary photons formed in the collimator walls and in the air around the target; this is shown by comparison of the background on the plates exposed to mesons to that of identical plates from a blank (no target) run. To go to smaller targets will involve precautions to remove this extra background.

The angular resolution of this experiment is determined partly by the amount of scattering in the absorbing materials, as we have said, but it is also affected by the angular width of the meson source as seen from the detector and by the width of the detector as seen from the source. In most cases the width of the scanned areas of the emulsion was about equal to the width of the meson source, so that these two source of angular width have approximately equal effects. The rms value of this angular width from both sources varied from about $\pm$ 5.6 to $\pm$ 1.9 degrees over the energy range at $\theta = 90^\circ$ and from about $\pm$ 3.9 to $\pm$ 1.6 degrees at 45° and at 135°. Combining these angular widths with that expected from scattering effects we find that the total root mean square angular uncertainties are about $\pm$ 7 degrees at $\theta = 90^\circ$ and about $\pm$ 6 degrees at 45° and at 135°. The scattering calculations were made using the method developed by Foldy.[5]

The energy resolution can be affected by several factors: thickness of the target, scattering in the absorber, widths of the target and of the scanned areas, and straggling due to energy loss fluctuations. At 90 degrees the only important factor is target thickness, and the rms energy uncertainty is a maximum of $\pm$ 4.0 Mev at the lowest energy observed and when calculated for the middle points of the various plates varies from $\pm$ 2.8 Mev down to

± 1.2 Mev at the highest energy observed. At 45 degrees and 135 degrees the edge of the copper absorber is at an angle of 45 degrees to the meson trajectory, and as a result uncertainties due to scattering in the absorber and to widths of the target and the scanned areas also become important. The resultant total rms energy uncertainty at 45 degrees and 135 degrees again calculated for the middle points of the plates is a maximum of ± 7.0 Mev at a meson energy of 150 Mev and decreases to ± 3.0 Mev at 33 Mev, the nominal energy at the middle of the plates of the first box.

C. Exposures

Three sets of plates were removed from the apparatus (and replaced with dummy plates) during the exposure run. These removals occurred at exposures of 3,400, 6,800, and 13,600 r, as would be measured at the position of the carbon target with an ionization chamber behind 1/8 inch of lead. Actually these numbers are extrapolated from the readings of the large ionization chamber situated in the beam some fifteen feet behind the carbon target. The sensitive chamber is an 8 inch cube. To find the actual number of equivalent r at the target, one multiplies the r reading of the chamber by the ratio of the chamber cross section to the beam cross section at the target (a factor of 212). This factor is necessary because the ionization chamber was calibrated with all of its volume exposed to radiation whereas the collimated beam fills only a fraction of the volume even after diverging from the target position.

The middle exposure, 6,800 r, was about optimum. Most of the plates scanned were from this batch. The exposure was limited by the darkening of the leading edges of the plates in the box with no absorber, even though this box was about twice as far from the target as the box in the next higher energy interval. In the batch of the highest exposure the plates of the

first box were practically unscannable. Even the plates of the next three boxes were scannable only with difficulty although these plates were somewhat shielded by the copper absorber from the electron shower. Incidentally, if lead had been used in place of the copper absorber, these plates would probably have had less background, except that the difficulty of the plates with no absorber would still have been present.

D. Examination of the Emulsions

The emulsions were scanned with standard microscopes for meson track endings. In most cases a total magnification of about 250 times (400 micron field of view) was used to locate the mesons, and a magnification of about 900 times (150 micron field of view) to examine each track in detail. In some cases of high background, it was necessary to use higher magnifications for searching. Altogether about 71 square centimeters of emulsion were scanned.

Meson track endings have in general two characteristics by which they can be recognized. One is a large amount of small angle scattering over the last one or two hundred microns of the track length. The other is a relatively fast change of grain density over the last 100 microns of the track length. These characteristics have meaning only relative to the characteristics of other tracks in the emulsion with which mesons might be confused. The only type of track with which a meson might be confused is that of a proton. Since the mass of the π-meson (276 electron mass units) is 1/6.65 times that of the proton, the multiple scattering of the meson is the larger. It turns out that for any given residual range (non-relativistic) the rms scattering per unit path of the meson is about 2.2 times more than that of the proton. Also since at a given velocity the meson and the proton lose energy by ionization at the same rate, the π-meson will go through the hump

of the Bragg ionization curve in 1/6.65 the distance that the proton takes, hence the characteristic rapid change of grain density at the end of a meson track.

Two other meson characteristics make the identification of some meson endings very easy. Most negative π-mesons produce stars at the ends of their tracks, and practically all positive π-mesons decay into μ-mesons at their track endings. Therefore any track which is observed to have stopped at a point where one or more different tracks are seen to start is almost certainly a meson ending. No other charged particle is known to produce a star-like phenomenon at the end of its range, barring, of course, such things as hammer tracks, which are easily recognized.

The interpretation of the various types of meson track endings found would have been very difficult if it had not been for the work of Gardner, Bradner, and co-workers with magnetically sorted mesons produced by the 184-inch Berkeley synchrocyclotron.

When a negative π-meson comes to rest in matter, it is virtually always captured by the positive nucleus of one of the surrounding atoms. Several thousand negative π-meson endings have been observed in emulsion without a definite negative π-μ decay's having been seen.[6] This puts an experimental upper limit of about 10^{-11} second for the mean life for the capture of negative π-mesons in C-2 emulsions, i.e., a factor of about 10^3 shorter than the mean life for π-μ decay.[7] The present theoretical picture of the capture process is consistent with the experimental evidence.[8] In being captured by a nucleus of atomic number greater than one, the negative π-meson reacts with a proton and with at least one other nucleon. The proton is transformed into a neutron, and it and the "other nucleon" share the kinetic energy supplied by the rest mass of the meson. The "other nucleon" is a

sort of catalyst; it does not change form in the reaction but is necessary to conserve momentum. It may be either a neutron or proton or even a group of nucleons. These reaction products may either (a) escape the nucleus, or (b) excite the nucleus by collision with other nucleons whereupon the nucleus will disintegrate according to the statistical model. Thus one might see under the microscope at the end of a negative π-meson track either (a) no ionizing track, or (b) one or more ionizing tracks. Meson endings of type (a) are called ρ-mesons; type (b) endings are called star endings and are abbreviated as σ-mesons (σ for star). In addition, either type may also have a blob of grains at the end of the meson probably indicating recoil of the residual nucleus. It should be added that this picture does not hold for the case of hydrogen as the capturing nucleus. From recent experiments by Panofsky, Aamodt, and York[9] the capture of a negative π-meson by an ordinary hydrogen atom is thought to result in the emission of gamma-rays, possibly through an intermediate process involving a neutral meson. However, no matter what the capture processes are in detail, the important fact for this experiment is the empirical result that in C-2 emulsions 73 (± 2) percent of negative π-mesons have σ-endings and the remaining 27 percent have ρ-endings.[10]

The characteristics of the track endings of negative μ-mesons are not as well known. White, Jones and Gardner[11] have found some 28 events thought to be endings of negative μ-mesons. Of these 26 are ρ-endings, and 2 are σ-types. These 2 σ-endings could very well have been due to negative π-meson contamination. There is good theoretical reason for expecting negative μ-mesons to have ρ-endings. From spin considerations (μ-mesons are thought to have half-integral spin), the negative μ-meson when captured is thought to react with a proton to form a neutron and a neutrino. The conservation of energy and momentum show that in such a reaction the neutron will get only

5.3 Mev kinetic energy, in which case the formation of a star is very unlikely. In matter of low atomic number ($Z < 10$) the capture time is so long that a negative μ-meson can also spontaneously decay, presumably into an electron and two neutrinos, in which case the track ending would again be a ρ-type.

Positive π-mesons almost always disappear via the π-μ decay route. When one comes to rest in matter near an atom it is repulsed by the Coulomb barrier and so does not get a chance to interact with a nucleon. The interaction with electrons is very weak. Experimentally it is observed that at least 99 percent of the positive π-mesons undergo π-μ decay.[12] Thus the positive π-meson track is known virtually always to end at the beginning of the lightly ionizing track of a positive μ-meson with about 4.1 Mev. Since the range of a 4.1 Mev μ-meson is about 600 microns and since the emulsion thickness is about 100 microns, the geometrical probability that the μ-meson will stay entirely within the emulsion is only about 8 percent. Scattering of the meson reduces this probability somewhat.

The track ending of a positive μ-meson is always a ρ-type because it too can only spontaneously decay. The decay products are a positron and two neutrinos,[13,14] none of which can be detected in C-2 type emulsion.

The types of track endings of the four kinds of mesons can be summarized in the following table:

TABLE I

Types of Meson Track Endings

Kind of Meson	Types of endings
Negative π	σ_n, ρ ($n = 1,2,3,\ldots$ = number of prongs)
Negative μ	ρ
Positive π	π-μ
Positive μ	ρ

It is seen that a ρ-ending can be interpreted as any of the three types of mesons and so is of little value by itself. There is another possibility of confusion in that a π-μ-ending of which only about 100 microns of the μ-track is seen resembles very much a σ_1-ending whose one prong is a lightly ionizing track. However in a study of 65 σ_1-endings in emulsions exposed to magnetically sorted negative π-mesons (kindly supplied by F. L. Adelman and S. B. Jones), it was found that most of the σ_1-endings with fast prongs had also recognizable "clubs," i.e., blobs of grains at the meson endings due presumably to recoil of the residual nuclei. It is known that π-μ-endings do not exhibit such "clubs." Of the 65 one prong stars, 14 had fast prongs and were possibly confusable with π-μ-endings. However, of the 14, only 2 did not exhibit recognizable "clubs." This means then, if we use the data of Adelman and Jones[10] on star prong distributions, that only about 1 percent of all σ-endings are confusable with π-μ-endings, provided one examines these tracks for "clubs."

From the discussion above we can interpret the various meson track endings in the following way:

(a) The number of σ-endings is equal to 1/.73 of the total number of negative π-meson endings.

(b) The number of π-μ-endings is equal to the number of positive π-meson endings.

(c) The ρ-endings are made up of (a) 0.27 of the negative π-meson endings and of (b) the positive μ-endings from the positive π-μ decay processes. Since the range of the μ-meson is only 600 microns, there should be as many positive μ-endings as positive π-endings in any sample volume, on the average. However, not as many of the μ-endings will be recognized partly because, being emitted isotropically

from the end of the π-mesons, many of them will be traveling at unfavorable angles for observation whereas most of the π-mesons are parallel to the plane of emulsion. Also since the μ-track on the end of a positive π-track acts like a label, the μ-ending is harder to recognize, especially if short, as it has no such label. No μ-mesons, neither negative nor positive, are expected from the carbon target. A previous experiment put an upper limit on the cross section for the production of pairs of μ-mesons as 0.02 ± .02 of the cross section for the production of positive and negative π-mesons.[15] This experiment allows a similar estimate to be made, as will be shown later. Only a negligible number of negative and positive μ-mesons are expected from π-μ decay processes in flight.

Meson endings which occur very near either surface of the emulsion are in danger of misinterpretation by an observer because, for example, one or more lightly ionizing particles might leave the emulsion before having produced enough developable grains to form recognizable tracks. To avoid these misinterpretations only meson endings 3 microns or greater from either surface after development were used in the calculations. The 3 micron criterion was established by plotting the frequency of each type of meson versus the distance to the nearest surface. It is seen from Figure 5 that the frequency is constant, within statistics, at distances of 3 microns or more. Since the 100 micron emulsion is only 40 microns in thickness after development, the above criterion removes 12.5 percent of the available emulsion volume.

The reliable observation of mesons in emulsions requires considerable experience. It was found that at least a month is necessary to train a new observer. Five observers worked on this experiment, three of which did the majority of the scanning. The absolute efficiency for the recognition of

mesons of four of these observers was determined by the duplicate scanning of certain areas of emulsion. All had efficiencies of greater than 90 percent for the recognition of σ- and π-μ-endings and from 80 to 95 percent for the recognition of ρ-endings. The fifth observer scanned only a small region and her efficiency was not checked absolutely; however, this observer was considered experienced and reliable, and her results agree with those obtained from adjacent areas of emulsion scanned by two of the other observers. As another means of comparing the observers and of minimizing their differences, each area of emulsion to be scanned was divided into three parallel sections, labeled A, B, and C in Figure 6, which were generally scanned by three different observers. The results of the three sections were plotted separately and found to be consistent within the limits of random sampling. After demonstrating in this way that no significant errors would be caused by individual observer differences, the data were collected irrespective of observer.

In many cases events were found in the emulsions that could not be classified at once with complete certainty. Each of these events was inspected by at least two experienced observers. This procedure generally resulted in complete agreement in interpretation. However, sometimes there was disagreement, in which case a vote was taken to decide its classification. Votes were necessary for only about 1 percent of the events found.

III. ANALYSIS OF DATA

A. Minus-plus Ratio

The ratio of the number of negative π-mesons to that of positive π-mesons produced in a certain meson energy range is, simply:

$$\frac{\pi^-}{\pi^+} = \frac{1.37\ \sigma}{\pi\text{-}\mu} \qquad \text{(III-1)}$$

where σ and π-μ represents the number of σ- and π-μ-endings, respectively, found in a volume of emulsion corresponding to the energy in question.

There is another analytical method for determining the minus-plus ratio which is a less reliable method but is of interest to indicate experimental consistency. The method is developed as follows. The number of negative π-mesons is again taken as $1.37\ \sigma$. Since only π-mesons are emitted from the target, the difference between the total number of mesons (T), including ρ-types, and the number of negative π-mesons is due to positive π- and μ-mesons. Taking $\pi^+ = \mu^+$ we get

$$\left(\frac{\pi^-}{\pi^+}\right)_{\text{alternate}} = \frac{1.37\ \sigma}{\frac{1}{2}(T - 1.37\ \sigma)} = \frac{2}{0.73\frac{T}{\sigma} - 1} \qquad \text{(III-2)}$$

B. Energy Spectrum

Consider a point source of mesons emitting $\frac{d^2N_o(E,\Theta)}{dEd\Omega}$ π-mesons per unit beam exposure per Mev per steradian at the polar angle Θ and with a kinetic energy E. Let a volume element of dimensions δ_1, δ_2, and δ_3 be imbedded in an absorbing medium at a distance R from the source and, for convenience, be oriented so that a $\delta_1\ \delta_2$ face of the volume is normal to the direction of R.

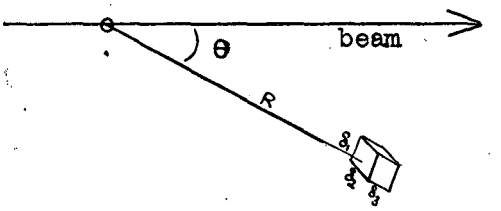

The number of π-mesons ($\triangle N$) stopping in this volume element will be

$$\triangle N = r \frac{d^2N_o(E,\theta)}{dEd\Omega} \frac{\delta_1\delta_2}{R^2} \delta_3 \frac{dE}{dR} \qquad \text{(III-3)}$$

where r is the number of units of beam exposure and $\frac{dE}{dR}$ is the rate of energy loss in the emulsion at energy E. If we write n, the meson density, for $\triangle N/\delta_1\delta_2\delta_3$, it becomes apparent that the numerical density of mesons, which is the basic microscope measurement, is independent of the exact size and orientation of the small volume element.

$$n \equiv \frac{\triangle N}{\delta_1\delta_2\delta_3} = r \frac{d^2N_o(E,\theta)}{dEd\Omega} \frac{1}{R^2} \frac{dE}{dR} \qquad \text{(III-4)}$$

To find the average density over a larger volume element we must use the mean value of the function $\frac{1}{R^2}\frac{dE}{dR}$ averaged over the volume element rather than its value at the center of the range interval. This function varies roughly as the inverse 2.5 power of R, and it can change as much as by a factor of 3.5 over the region of one plate. Thus the average value of the emission function at each point is found from

$$\left[\frac{d^2N_o(E,\theta)}{dEd\Omega}\right]_{av} = \frac{1}{r} \frac{n}{\left(\frac{1}{R^2}\frac{dE}{dR}\right)_{av}} \qquad \text{(III-5)}$$

One might ask what effects can distort the emission spectrum measured in this way. One possible effect is π-μ decay in flight, but the time of flight in the air between the carbon target and the absorbing medium plus the slow down time in the absorber is so fast that only about 3 percent of

the π-mesons decay before coming to rest. This time interval as measured in the meson's system varies from 2 to 3 x 10^{-10} second over the energy spectrum at 90°. Although this loss of mesons is negligibly small, it is interesting that the loss is roughly constant with energy so that the relative shape of the emitted spectrum is affected less than the absolute magnitude. It would be very difficult to identify a π-μ decay in flight in an emulsion, and none is expected to be observed.

Another distorting effect is the nuclear absorption of the mesons while traversing the absorber. The cross section for this process at low meson energies is not known and it cannot be corrected for accurately at this time. However, we might put an upper limit on the effect of this process by assuming that the cross section is equal to the nuclear area as measured by 90 Mev neutrons.[16] Then the mean free path in copper is 10.7 cm, and the absorption between 17 Mev and 55 Mev (which is near the maximum of the 90° spectrum) is about 15 percent, and the absorption between 17 Mev and 100 Mev is about 30 percent. For π-mesons having energies of "some hundred Mev" Piccioni[17] gives an experimental lower limit for the mean free path for nuclear absorption as 1200 grams per square centimeter (135 centimeters of copper). Using this, the only measured value, we find that the nuclear absorption between 17 Mev and 100 Mev is only 3 percent, negligible in this experiment. If in addition to nuclear absorption there were nuclear scattering in which mesons can be scattered through large angles, and if the experiment were done with poor geometry in the detection system, as in this experiment, the scattered mesons would be detected at distances from the source which are much less than their actual ranges. This effect could conceivably cause an emitted spectrum which, for example, is constant in energy out to a maximum energy to be measured as one with a hump at some intermediate energy. This false hump might be avoided

by the acceptance of only those mesons within a certain angular range. This process is not likely, however, as nuclear scattering of greater than 90° would have been measured by Piccioni as nuclear "absorption" in his experiments on high energy mesons.

The measured emission spectrum could be distorted also if the approximation of a point source were not valid. In the formula for the emission function one should calculate the mean of the function

$$\frac{1}{R^2} \frac{dE}{dR}$$

over the volume of a finite target. However, since a tedious numerical integration was indicated, just the mean of the most rapidly varying part, the sub-function $\frac{1}{R^2}$, was calculated as a first approximation. It turns out that the ratio

$$\frac{(1/R^2)_{mean}}{(1/R_o^2)} = 1 + 1/5\ (a/R_o)^2 + \ldots \qquad \text{(III-6)}$$

where R_o is the distance from the detector to the center of the target and a is the radius of the spherical target. For the worst case in the experiment this ratio differs from unity by only 1 percent. Thus the point source approximation was justified for the target used.

To find out whether any of the mesons observed might have come from sources other than the carbon target a blank run was made, that is, a run identical to the main run except that the carbon target was omitted. No mesons at all were found in areas which in the main run would have yielded about 130 mesons.

C. Cross Section Computations

If one assumes the existence of some functional relationship between E, θ and k, where k is the energy of the photon creating the meson of energy

E at angle θ, we can relate the emission spectrum to a differential cross section:

$$\frac{d^2N_o(E,\theta)}{dEd\Omega} = \int N(k,r) \frac{d\sigma(k,\theta)}{d\Omega} (\partial k/\partial E)_\theta \, n_t \, dV(r) \quad \text{(III-7)}$$

where $N(k,r)$ = the integrated number of photons of energy k per Mev per unit beam exposure per square centimeter of beam area at radius r from the beam axis at the target,

$\frac{d\sigma(k,\theta)}{d\Omega}$ = cross section for the production of meson per steradian at angle θ by a photon of energy k in cm^2 per nucleus,

n_t = numerical density of the target atoms in cm^{-3},

and $dV(r)$ = element of target volume at radius r from the beam axis in cm^3.

The integral is to be taken over the target volume.

There are various collision models one might assume in order to compute $(\partial k/\partial E)_\theta$. For example the assumption that only two particles (a meson and a residual nucleus) result from the photon-nucleus collision plus the application of conservation laws allows us to compute such a function. This case also gives us, incidentally, the maximum possible meson energy at each angle for any given photon energy. Another example is the model in which just three particles result from the collision, a meson, a nucleon, and a residual nucleus; however, the momentum of one of these three particles must be specified before that of the others can be determined. Plausible supplementary assumptions then are that the residual nucleus is at rest (a) in the laboratory system or (b) in the zero-momentum system of the photon-nucleus collision. Curves of E vs k for these three cases are plotted in Figure 7.

The function $N(k,r)$ is known, so that we can write

$$\frac{d\sigma(k,\theta)}{d\Omega} = \frac{d^2N_o(E,\theta)}{dEd\Omega} \left(\frac{\partial E}{\partial k}\right)_\theta \frac{1}{V \, n_t \, \bar{N}(k)} \quad \text{(III-8)}$$

where $\bar{N}(k)$ is the mean value of $N(k,r)$ averaged over the volume of the target (V). It turns out that $\bar{N}(k)$ for the spherical target used equals 1.04 times the mean value of $N(k,r)$ averaged over the beam cross section at the target. The shape of the beam over the target is shown in Figure 8. It was assumed that the composition of the beam in energy was independent of r over the region used.

A cross section that can be computed without reference to any particular collision model is the average cross section per steradian over the x-ray energy spectrum. Integrating equation (III-7) over the meson spectrum at constant angle θ, we get:

$$\frac{d\,N_o(\theta)}{d\Omega} = \int_o^{E_{max}} \frac{d^2N_o(E,\theta)}{dE d\Omega}\,dE = n_t\,V \int_o^{E_{max}} \frac{d\sigma(k,\theta)}{d\Omega}\,\bar{N}(k)\left(\frac{\partial k}{\partial E}\right)_\theta dE$$

$$\frac{d\,N_o(\theta)}{d\Omega} = n_t\,V\,\frac{d\bar{\sigma}(\theta)}{d\Omega}\int_{k_{min}}^{k_{max}} \bar{N}(k)\,dk$$

$$\frac{d\,N_o(\theta)}{d\Omega} = n_t\,V\,\frac{d\bar{\sigma}(\theta)}{d\Omega}\,q \qquad \text{(III-9)}$$

where $\frac{d\bar{\sigma}(\theta)}{d\Omega}$ is the mean differential cross section averaged over the photon spectrum, and q represents the indicated integral. Thus we get

$$\frac{d\bar{\sigma}(\theta)}{d\Omega} = \frac{d\,N_o(\theta)}{d\Omega}\,\frac{1}{q\,n_t\,V} \qquad \text{(III-10)}$$

The number q is not clear cut. As a first approximation $\bar{N}(k)$ varies as

$$\bar{N}(k) = A/k \qquad \text{(III-11)}$$

where A is a constant so that

$$q' = A\int_{k_{min}}^{k_{max}} \frac{dk}{k} = A\,\ln\frac{k_{max}}{k_{min}} \qquad \text{(III-12)}$$

However, it is equally proper to use the convention of defining the number of quanta in a bremsstrahlung spectrum as equal to the total energy in the beam divided by the maximum energy.

$$q = \frac{\text{total energy}}{k_{max}} = \frac{1}{k_{max}} \int_0^{k_{max}} k\, \bar{N}(k)\, dk \qquad \text{(III-13)}$$

This definition is unique, and it avoids the divergence in the number of quanta near zero energy. Furthermore, it avoids the approximation involved in equation (III-11) and it avoids also the determination of the threshold energy k_{min}. If, e.g., the actual spectrum had the shape given by equation (III-11), this definition would make the number of quanta equal to the constant A. The number q is the number of photons per square centimeter averaged over the volume of the target. The total number of quanta in the "one-half inch" beam of the Berkeley synchrotron has been determined experimentally by Blocker, Kenney, and Panofsky[18] to be 1.5×10^{10} ($\pm$ 35 percent) quanta per r, where the r is the unit of exposure as measured by the large ionization chamber used to monitor the beam.

Having now obtained the average cross section per steradian over the x-ray spectrum, one can get the average total cross section ($\bar{\sigma}_t$), by integrating it over all angular space:

$$\bar{\sigma}_t = \int \frac{d\bar{\sigma}(\theta)}{d\Omega}\, d\Omega$$

$$\bar{\sigma}_t = 2\pi \int_0^{\pi} \frac{d\bar{\sigma}(\theta)}{d\Omega} \sin\theta\, d\theta \qquad \text{(III-14)}$$

$\frac{d\bar{\sigma}(\theta)}{d\Omega}$ was measured at 3 angles, 45°, 90°, and 135°, so one must extrapolate below 45° and above 135°. Fortunately, however, the sin θ factor minimizes errors in these regions.

IV. RESULTS

A. Minus-plus Ratio

The ratio of the number of negative π-mesons to the number of positive π-mesons in each energy interval for the three values of the angle θ are shown in Figure 9. The errors plotted with the experimental points are standard statistical errors. The theoretical ratio for photon-nucleon collisions as determined by Brueckner and Goldberger[19,20] for the case in which the interaction between a neutron and a photon is negligible is a function of both energy and angle, and these values are shown on the same figure, including the Coulomb effect of a distributed charge. The expression for the theoretical ratio, without the Coulomb effect, is

$$\pi^-/\pi^+ = \left[1 - \frac{E_T}{Mc^2}\left(1 - \frac{v}{c}\cos\theta\right)\right]^{-2}$$

where E_T represents the total meson energy, including rest energy, v the meson velocity, c the velocity of light, and Mc^2 the rest energy of a nucleon.

At $\theta = 45^\circ$ there is a possible variation of the experimental ratio with energy, but the points are also statistically consistent with a constant ratio independent of energy. There is no disagreement with the theory here as the theory calls for a ratio which is practically constant over the energy range examined.

At $\theta = 90^\circ$ and 135° there is again no statistically significant variation of the experimental ratio with energy, except for the fact that the lowest energy points consistently have a value near 2. Although the Coulomb effect at the energies designated should be very low, those high values of the ratio possibly do represent the Coulomb effect. The designated energies assume that the mesons come from the middle of the carbon target, whereas it is possible that an appreciable number of the mesons come from the surface

region of the target with energies at which the Coulomb effect is important. At $\theta = 90^{\circ}$ the experimental points do not agree very well with the theory, but with the statistics involved one cannot state that the difference is significant. However, at $\theta = 135^{\circ}$ the discrepancy between theory and experiment is more distinct and appears to be significant.

Since in each case the experimental data are statistically consistent with a constant value of the minus-plus ratio, the data were lumped together to determine the overall minus-plus ratio at each angle. These values are given in Table II, and plotted in Figure 10 together with the mean theoretical values found by weighting theoretical value at each energy interval with the number of mesons found in that interval. The mean energy determined similarly is listed also. The alternate, less reliable, method of computing the minus-plus ratio, discussed in Section III-A, which uses the total number of mesons, was applied to the data also for the purpose of comparing the methods. It should be added that if one plots and integrates the negative and positive energy spectra separately and thus obtains the minus-plus ratios, the results agree well with those obtained by considering the ratio to be independent of energy.

TABLE II

Overall Minus-plus Ratio versus Angle of Emission

Angle	Experimental Ratio	Weighted Theoretical Ratio	Mean Energy	Experimental Ratio (Alternate Method)
45°	1.29 ± .22	1.25	70 Mev	1.60
90°	1.30 ± .12	1.62	56 Mev	1.60
135°	1.34 ± .20	2.12	54 Mev	1.32

These overall ratio results again point out the discrepancy between theory and experiment. The experimental ratio appears to be independent of angle, as well as energy, whereas the theoretical ratio is not. This discrepancy might be explained by scattering of the mesons before they escape the carbon nuclei in which they are formed. This effect would make all characteristics of the emission spectrum isotropic. However, this explanation does not hold as the experimental energy spectra do depend on the angle of emission. A better explanation is, as indicated in Brueckner's analysis,[20] that the experimental results show the assumption (negligible neutron-photon interaction) of this form of the theory to be wrong and that the interaction of the neutron with the electromagnetic field through its magnetic moment does play an important part in the process.

One disturbing aspect of these results is that they disagree with that of a previous experiment which gave an overall ratio of 1.7 ± 0.2 at an angle of 90°.[3] The previous experiment differed from the present one mainly in that a line target was used and in that the angular resolution was about $\pm 45^{\circ}$. The discrepancy between the old and new results is greater than that allowed by the statistical errors. However, the new result is believed to be the more reliable.

B. Energy Spectra and Cross Sections

The spectra of π-mesons emitted from the carbon target were computed from the data using the total number of π-mesons, both negative and positive, at each energy interval. That is, it was assumed that the minus-plus ratio was independent of energy, as indicated in the last section. If one actually plots the negative and positive spectra separately, no statistically significant distinction appears in their relative shapes.

The emission spectra for 45°, 90°, and 135° are shown in Figures 11,

12, and 13, respectively. Smooth curves are drawn through the experimental points and extrapolated to zero energy for the purpose of obtaining the total number of mesons emitted at each direction. In Figure 14 the three smooth curves are drawn together for the purpose of intercomparing the three spectra.

Comparison of the spectra with Figure 7, which relates photon energy, meson energy, and angle of emission for three collision models, shows that the fundamental process in the formation of mesons is probably a photon-nucleon collision, as was expected, rather than a photon-nucleus collision. This is indicated both by the magnitude of the maximum energies of the spectra and by the amount of angular dependence. This angular dependence can of course be explained on purely kinematical grounds. The end points are not precise, but rather the spectra seem to have high energy tails which are attributable to the internal motion inside the carbon nucleus.

Another result is that fewer mesons are emitted in the forward direction than at 90° and probably fewer even than at 135°. Integrals of the spectra lead to values of the average cross section per steradian listed in Table III.

TABLE III

Average Cross Sections per Steradian

Emission Angle	$d\bar{\sigma}/d\Omega$ cm^2 per steradian per nucleus per photon
45°	$(2.42 \pm .21) \times 10^{-29}$
90°	$(3.75 \pm .17) \times 10^{-29}$
135°	$(2.75 \pm .20) \times 10^{-29}$

The errors listed are purely statistical errors. There is also a systematic error of about ± 35 percent due to an uncertainty in the absolute calibration of the number of quanta in the beam, but it does not effect the relative validity of the cross sections given.

The lack of a strong forward peak which would be predicted by classical electromagnetic theory if the interaction were that of an electric dipole effect has already been pointed out by Steinberger and Bishop[21] in a preliminary study on positive photomesons produced in hydrogen.* These workers investigated the angular dependence of only one photon energy in this work. It can be determined whether the binding of the nucleons in the carbon nucleus plays an important role in the angular dependence of the emitted spectrum when more complete data are available for the hydrogen case. The binding apparently plays a role in the shape of the energy spectrum, as results at 90° indicate that the hydrogen spectrum is considerably flatter than the carbon.

The effect of the binding of the nucleons is evidenced most strongly in the magnitude of the cross section. Comparison of these results at 90° with those of Cook from liquid hydrogen shows that the cross section per nucleus for the production of positive mesons from carbon is only about twice that from hydrogen, although there are six times as many protons in the carbon nucleus. This result checks a previous result of Steinberger and Bishop.[16]

The differential cross section per steradian as a function of the photon energy was not computed because it was felt that the details of the photon-nucleon collision were not known well enough to make such a calculation meaningful.

The cross section figures per steradian listed in Table II are also plotted in Figure 15. The smooth curve in the figure was drawn in to obtain the total average cross section integrated over all angles according to equation III-15. The resultant figure is 3.9×10^{-28} cm^2 per nucleus per

---

* The work with hydrogen has been done by L. J. Cook with nuclear emulsions and by J. Steinberger and A. S. Bishop with counter techniques. I am indebted to them for the use of some of their results before publication.

photon. The total uncertainty in this figure is due largely to the uncertainty in the absolute calibration of the beam in terms of the monitor used and is estimated to be about ± 40 percent.

C. Angular Distributions of the Mesons

The angular distributions of the mesons found at the emission angle of 90° are plotted in Figure 16. The angle of each meson is measured at the point where it enters the emulsion. The projected track lengths in emulsion ranged from 25 to 4000 microns, but the bulk of them lay in the 100 to 200 micron interval, as shown in Figure 17. The amount of multiple Coulomb scattering expected depends upon the initial energy of the meson, upon the energy at the point where the angle is observed, and upon how much its trajectory lies in glass and how much in copper. Choosing mesons which end near the middle of the plates with residual ranges of 200 microns as typical, one finds that the rms angle of scatter varies from 14° to 21° over the energy range covered as is in the neighborhood of 18° where most of the mesons were found.

Both the σ-meson and the π-μ-meson plots of Figure 16 give half widths of 17.5 degrees at half amplitude in good agreement with the above discussion.

The distribution of the angles at which the μ-mesons leave the end of the positive π-mesons (measured with respect to the beam direction) is clearly isotropic within the statistics involved. That the μ-mesons are isotropic also with respect to the angle to the normal to the emulsion plane is shown by the track length distribution of the μ-mesons in Figure 17. The smooth curve is the theoretical curve for isotropic emission from points uniformly distributed throughout the scanned volume.

The plot of the angular distribution of the ρ-mesons is clearly composite, being composed of a peak at 90° due to negative π-mesons which do

not make stars and a flat background due to positive μ-mesons whose beginnings are not observed. It can be seen that the height of the flat background is only about half the height of the μ-meson plot. A more detailed examination of these plots allows one to estimate that the positive μ-meson is on the average only 0.6 times as easy to recognize as the positive π-meson in 100 micron C-2 emulsions. One can also find the fraction of the negative π-mesons which do not form stars by comparing the number of mesons under the hump of the ρ-meson plot (after subtracting off the flat background) with the number of σ-mesons on the plot above, taking into account the number of σ-mesons in the 180° to 360° interval. This fraction turns out to be $0.31 \pm .07$, the error being purely statistical. This value compares well with the value $0.27 \pm .02$ found by Adelman and Jones[10] with magnetically sorted negative mesons. The angular width of this hump is again about 17.5 degrees.

If μ-mesons were formed in the target they would appear as ρ-mesons in the plates and would contribute to the hump in the ρ-meson angular distribution. If we use 0.27 as the real fraction of negative π-mesons which do not form visible stars, we can again use the number of ρ-mesons in the hump to determine an upper limit on the cross section for the production of μ-mesons. By subtracting from this group of ρ-mesons 0.27 times the total number of negative π-mesons, as determined by the number of σ-mesons in the same angular range, we obtain a residual number of ρ-mesons possibly attributable to μ-mesons from the target. If we assume that the μ-mesons are produced in pairs, we thus find that the ratio of the cross section for μ-meson production to that for negative plus positive π-meson production is 0.02 ± 0.02; the error is statistical.

The angular plots for emission angles of 45° and 135° correspond very well with those obtained at 90°; but they are less conclusive as fewer mesons were counted there. For completeness, these plots are shown in Figures 18 and 19.

V. ACKNOWLEDGMENTS

It is a pleasure to acknowledge the continued guidance and support of Professor E. M. McMillan. I wish to thank also R. S. White and W. S. Gilbert for cooperation throughout the experiment, Mrs. Edith Goodwin and Mrs. Hazel Gaffey for help in the microscope work, Drs. E. Gardner and H. Bradner and co-workers for the use of the facilities of the Radiation Laboratory Film Program and for many helpful discussions, Mr. W. Salsig for the mechanical design, and Mr. W. D. Gibbins and other members of the synchrotron crew for cooperation and helpfulness above and beyond the call of duty.

I wish to dedicate this thesis to my wife Beverly, whose continued encouragement has meant much to its completion.

VI. REFERENCES

(1) E. M. McMillan and J. M. Peterson, "Production of Mesons by X-rays," Science, 109 (1949), 438.

(2) J. Ise, Jr. and W. B. Fretter, "Extensive Penetrating Cosmic Ray-Showers," Physical Review, 76 (1949), 933.

(3) E. M. McMillan, J. M. Peterson, and R. S. White, "Production of Mesons by X-rays," Science, 110 (1950), 579.

(4) J. Steinberger and A. S. Bishop, "The Detection of Artificially Produced Photomesons with Counters," UCRL-631, March 1950.

(5) L. L. Foldy, "Multiple Scattering with Energy Loss," Physical Review, 75 (1949), 311.

(6) H. Bradner, "Review of Work on Artifically Produced Mesons," UCRL-486, October 1949, 39.

(7) E. A. Martinelli and W. K. H. Panofsky, "Lifetime of the Positive π-Meson," Physical Review, 77 (1950), 465.

(8) R. E. Marshak and A. S. Wightman, "Absorption of Negative π-mesons by Protons," Physical Review, 76 (1949), 114.

(9) W. K. H. Panofsky, L. Aamodt, and H. F. York, "The Gamma Ray Spectrum from the Absorption of π^--Mesons in Hydrogen," UCRL-673, April 1950.

(10) F. L. Adelman and S. B. Jones, "Stars in Photographic Emulsions Initiated by π^--Mesons," UCRL-530, November 1949.

(11) S. B. Jones and R. S. White, "Relative Energy Distributions of Low Energy π^-mesons from 390 Mev Alpha Particles on Carbon and Some Information about μ^--mesons," to be published.

(12) F. M. Smith, private communication.

(13) R. B. Leighton, C. D. Anderson, and A. Seriff, "The Energy Spectrum of the Decay Particles and the Mass and Spin of the Mesotron," Physical Review, 75 (1949), 1432.

(14) J. Steinberger, "On the Range of the Electrons in Meson Decay," Physical Review, 75 (1949), 1136.

(15) E. M. McMillan, J. M. Peterson, and R. S. White, unpublished data.

(16) L. J. Cook, E. M. McMillan, J. M. Peterson, and D. C. Sewell, "Total Cross Sections of Nuclei for 90 Mev Neutrons," Physical Review, 75 (1949), 7.

(17) O. Piccioni, "On the Secondary Particles of Local Penetrating Showers," Physical Review, 77 (1950), 6.

(18) W. Blocker, R. Kenney, and W. K. H. Panofsky, "Transition Curves of 330 Mev Bremsstrahlung," UCRL-565, March 1950.

(19) K. A. Brueckner and M. L. Goldberger, "The Excess of Negative over Positive Mesons Produced by High Energy Photons," Physical Review, 76 (1949), 1725.

(20) K. A. Brueckner, "The Production of Mesons by Photons," UCRL-597, February 1950 (to be published in Physical Review).

(21) J. Steinberger and A. S. Bishop, "Preliminary Results on the Production of Mesons by Photons on Carbon and Hydrogen," UCRL-632, March 1950.

VII. ILLUSTRATIONS

Figure Captions

Figure 1: Schematic drawing showing the essential experimental components.

Figure 2: A. Scale drawing of a longitudinal view of the collimator-target-detector assembly.

B. Scale drawing of a cross sectional view of the target-detector assembly.

Figure 3: Photograph of the experimental arrangement. The x-ray beam emerges from the synchrotron at A. B is the primary lead collimator. C is the copper absorber. Copper boxes containing the nuclear plates fit into the longitudinal slots. The x-ray beam emerges from this assembly at D.

Figure 4: Close-up photograph of target-detector assembly looking along the beam toward the synchrotron. The carbon target is seen at A. B is the box of plates in the key-hole (zero absorber) slot. Most of the copper absorber cannot be seen because of the duraluminum end plate C.

Figure 5: Depth distributions of the three types of mesons found. Data from all angles are included.

Figure 6: Drawing illustrating method of selecting areas of emulsion to be scanned.

Figure 7: Relations between photon energy, meson energy, and angle of emission in the laboratory system for three collision models derived from conservation laws. Supplementary assumption for models 2 and 3 was that the residual nucleus $_5B^{11}$ was at rest

(2) in the zero momentum system of the photon-$_6C^{12}$ system and (3) in the laboratory system.

Figure 8: Plot of the beam intensity at the target position against radius from the beam axis.

Figure 9: Plots of the experimental minus-plus ratio against meson energy for three angles of emission. The theoretical curve is for the case in which the neutron-photon interaction is negligible; the Coulomb effect of a distributed charge is included.

Figure 10: Plot of the mean minus-plus ratio averaged over energy versus angle of emission, using the data of Figure 9.

Figure 11: Experimental energy spectrum of positive and negative π-mesons emitted at 45° to the beam direction in units of mesons per Mev per steradian per r, where an r represents a unit reading of the large ionization chamber.

Figure 12: Experimental energy spectrum of positive and negative π-mesons emitted at 90° to the beam direction. The indicated error for the point with zero ordinate was taken as that due to one meson.

Figure 13: Experimental energy spectrum of positive and negative π-mesons emitted at 135° to the beam direction.

Figure 14: An intercomparison of the three energy spectra.

Figure 15: Plot of the average cross section per steradian versus angle of emission. The smooth curve was drawn for the purpose of integration.

Figure 16. Angular distributions of the mesons found at 90°. The abscissa is the angle from the beam direction.

Figure 17: Distributions in projected track length in emulsion for four types of mesons. Data from all angles are included. The track length measurements are estimated to be accurate to within 10 percent.

Figure 18: Angular distributions of the mesons found at 45°.

Figure 19: Angular distributions of the mesons found at 135°.

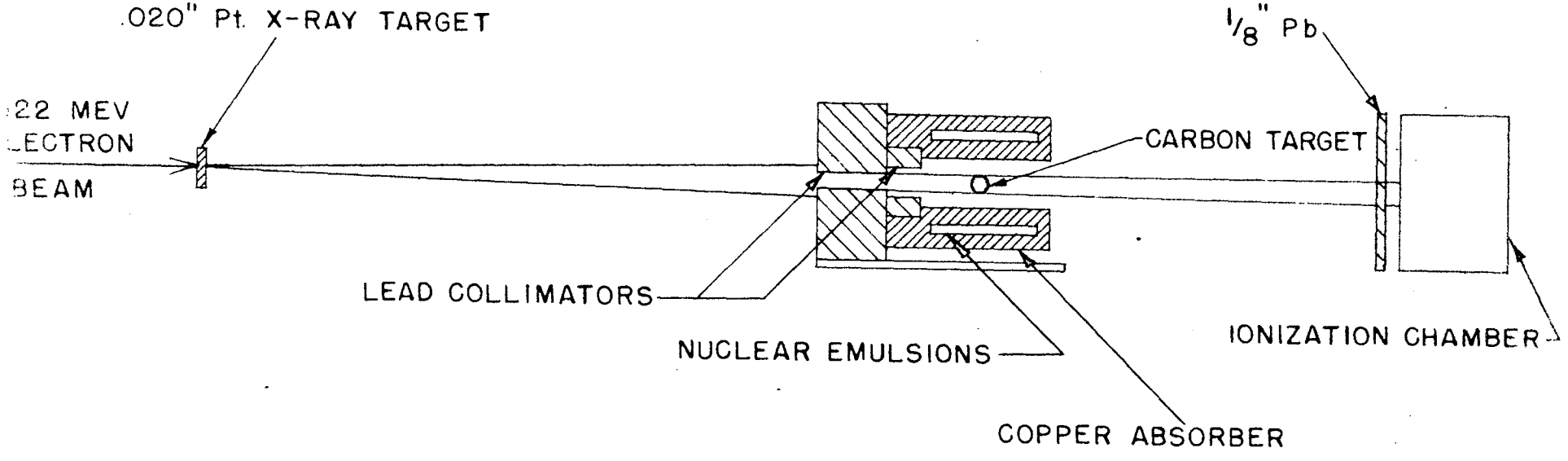

EXPERIMENTAL ARRANGEMENT

Fig. 1

14910-1

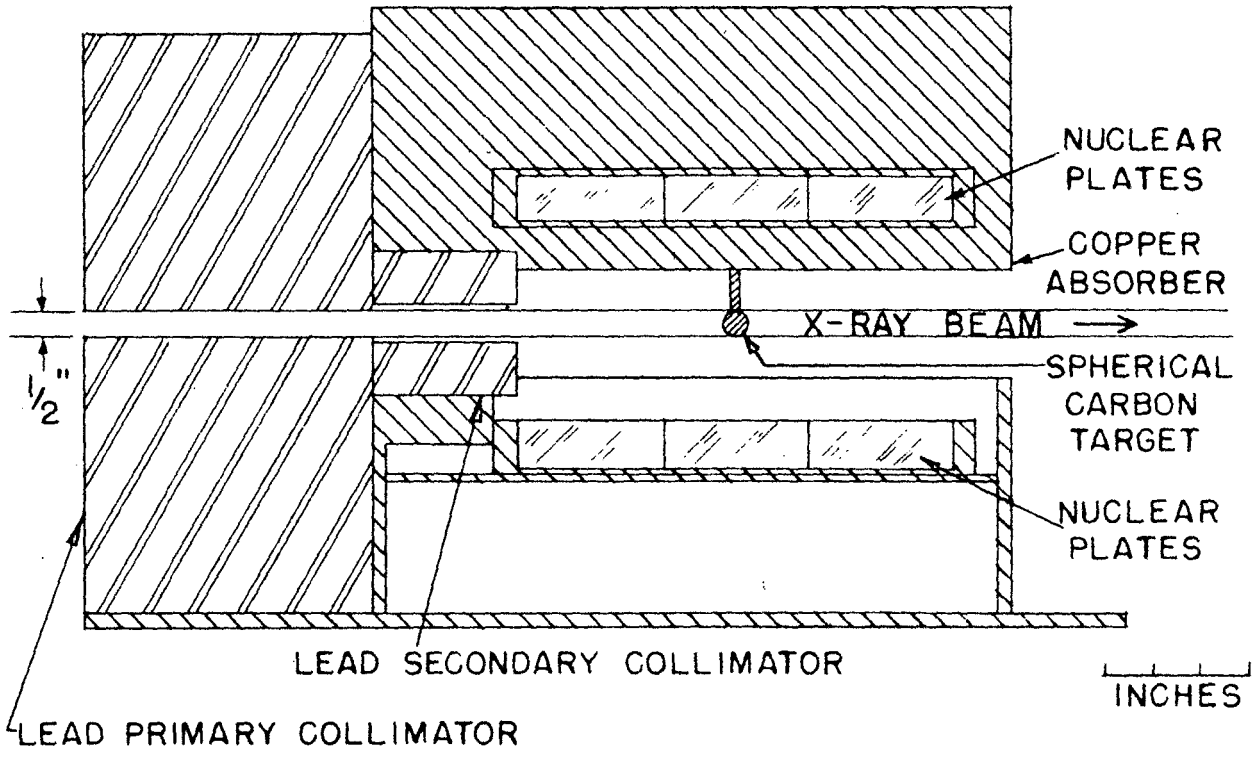

A. COLLIMATOR – TARGET – DETECTOR ASSEMBLY, LONGITUDINAL VIEW (¼ SCALE)

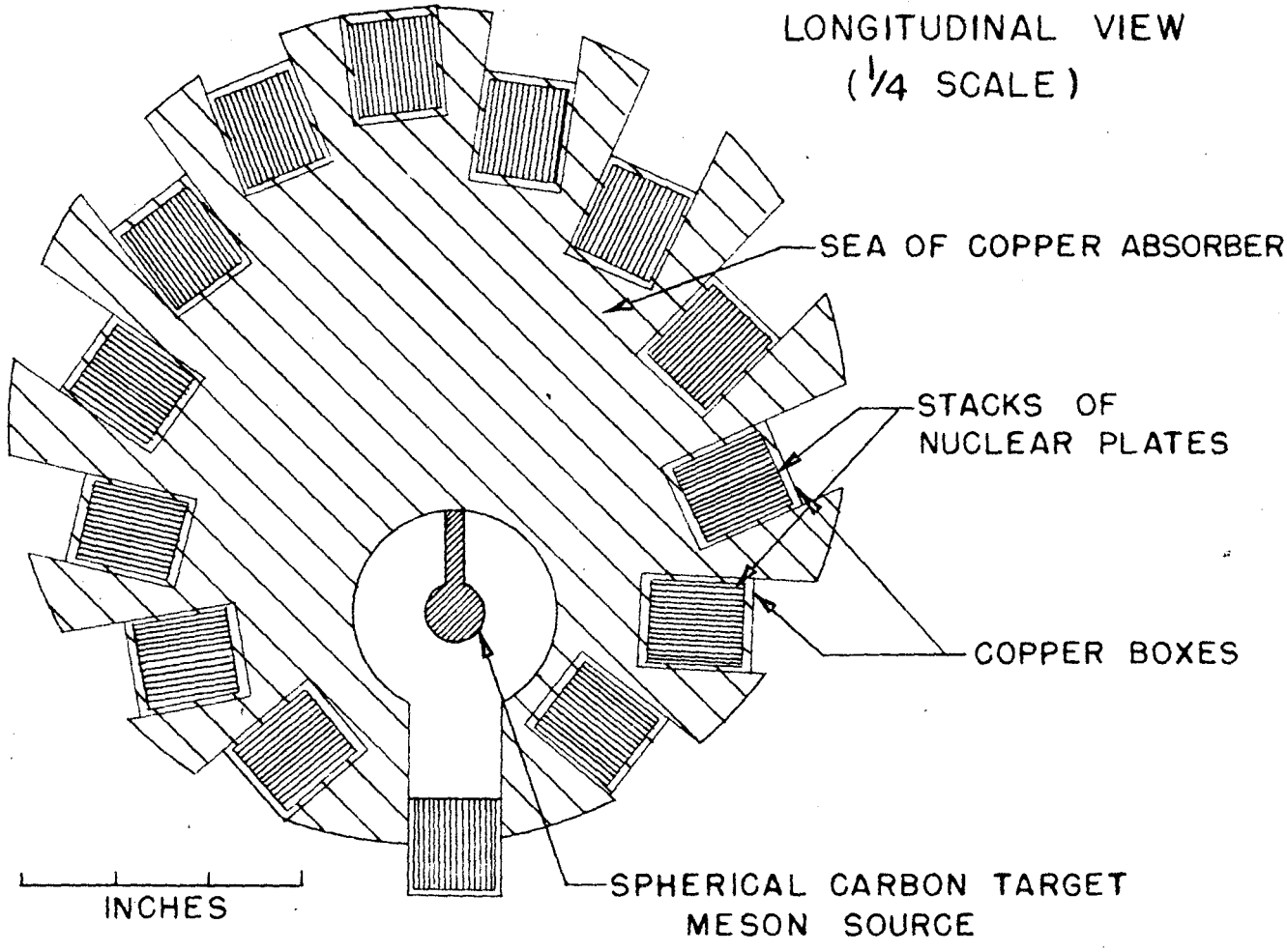

B. TARGET – DETECTOR ASSEMBLY, CROSS SECTION VIEW (½ SCALE)

Fig. 2

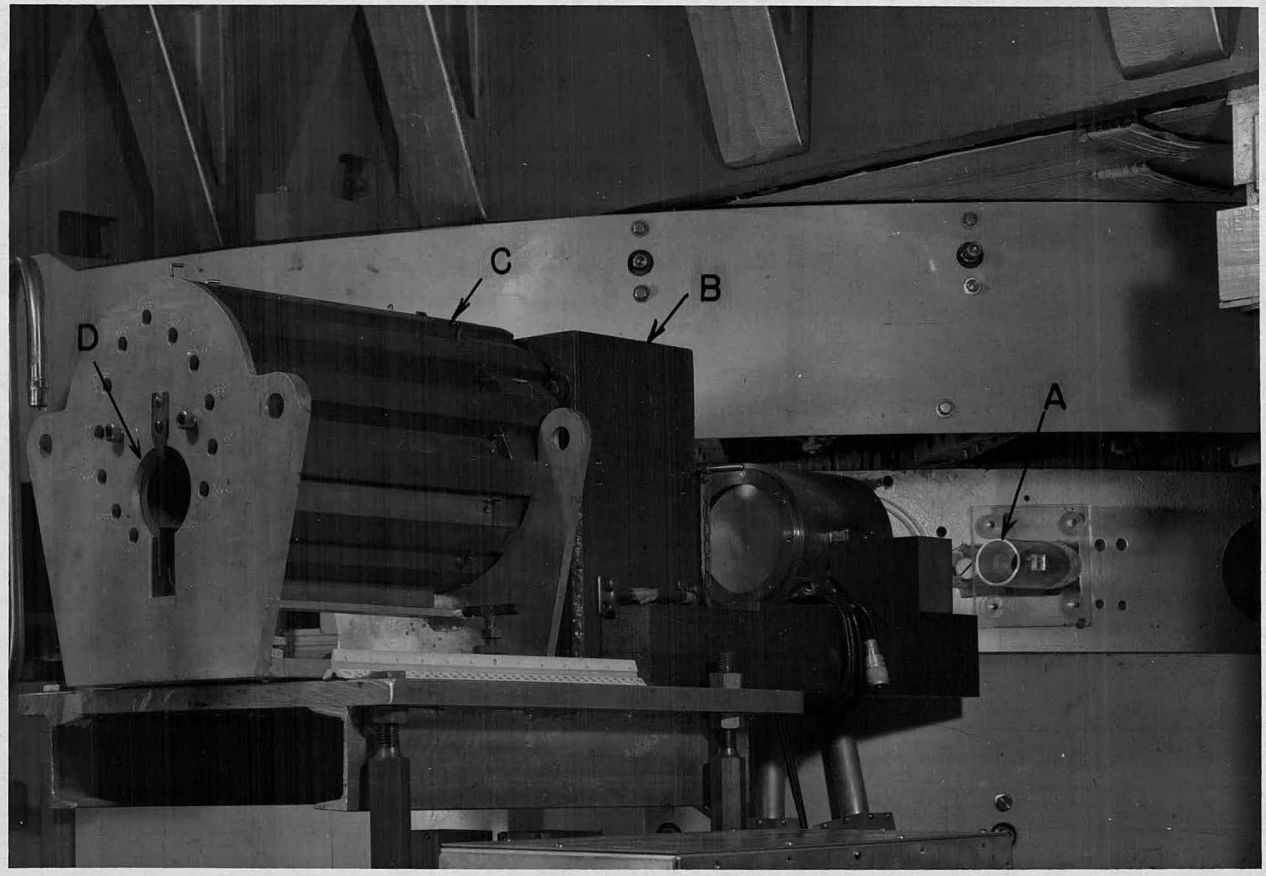

FIG. 3

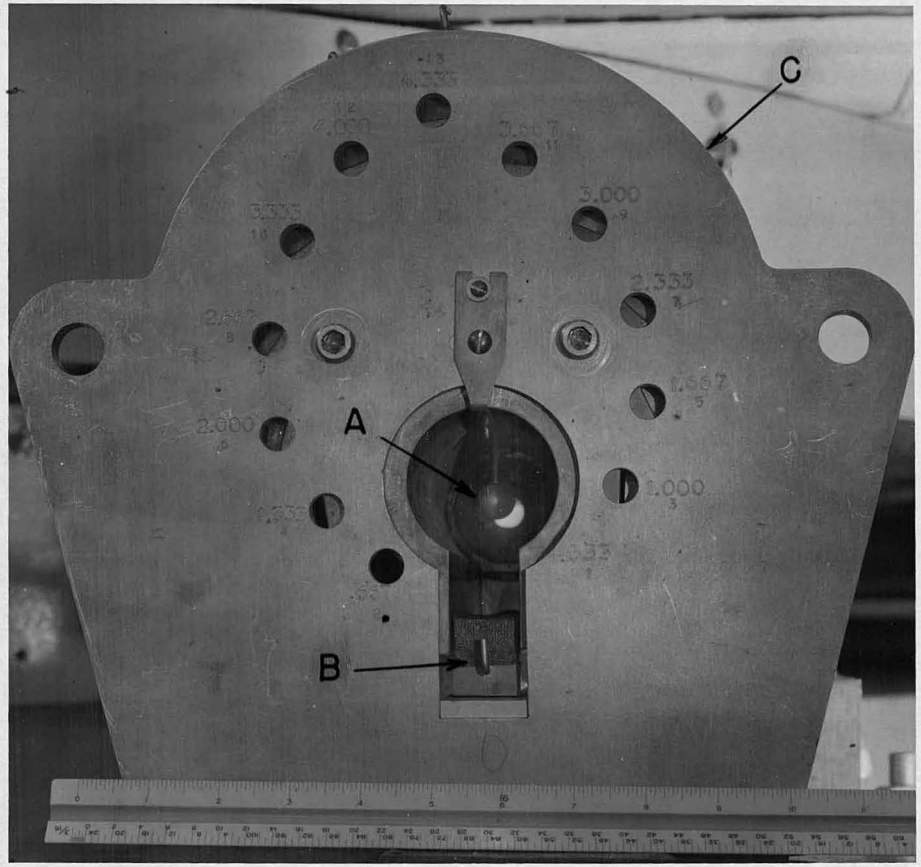

FIG. 4

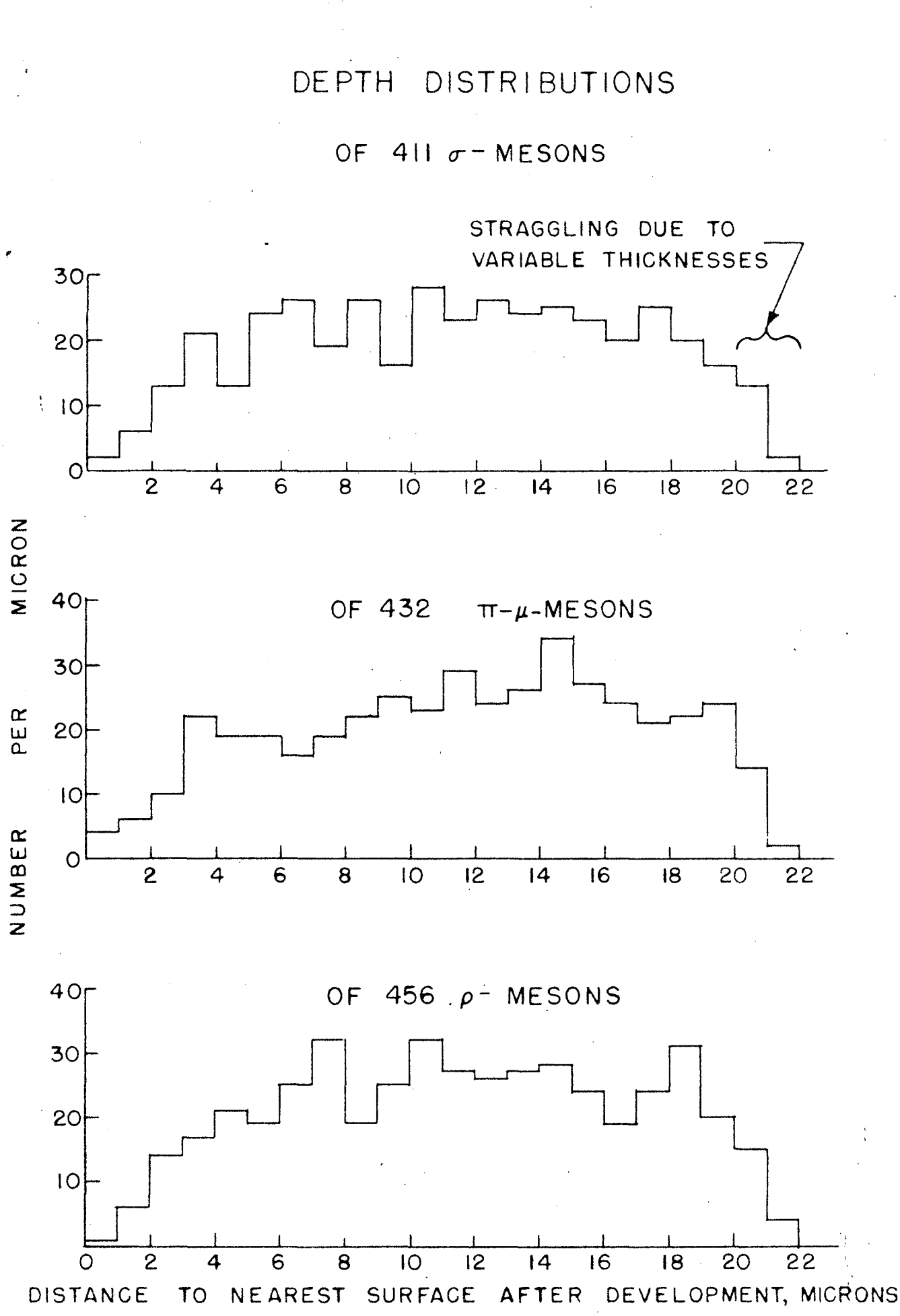
DEPTH DISTRIBUTIONS
OF 411 σ⁻ MESONS
STRAGGLING DUE TO
VARIABLE THICKNESSES
OF 432 π-μ-MESONS
OF 456 ρ⁻ MESONS
NUMBER PER MICRON
DISTANCE TO NEAREST SURFACE AFTER DEVELOPMENT, MICRONS

Fig. 5

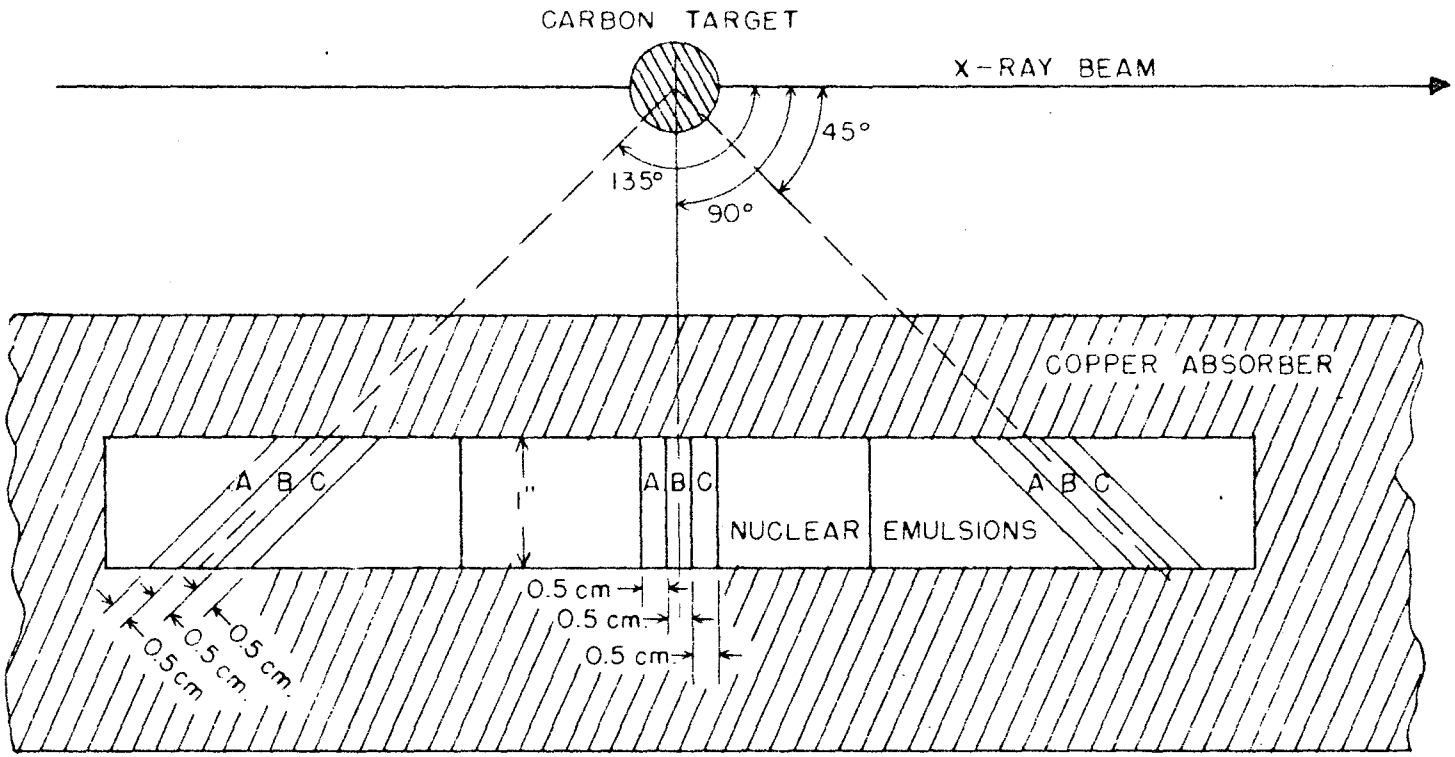

AREAS OF EMULSIONS SELECTED FOR SCANNING

Fig. 6

PLOT OF BEAM INTENSITY AT THE TARGET POSITION

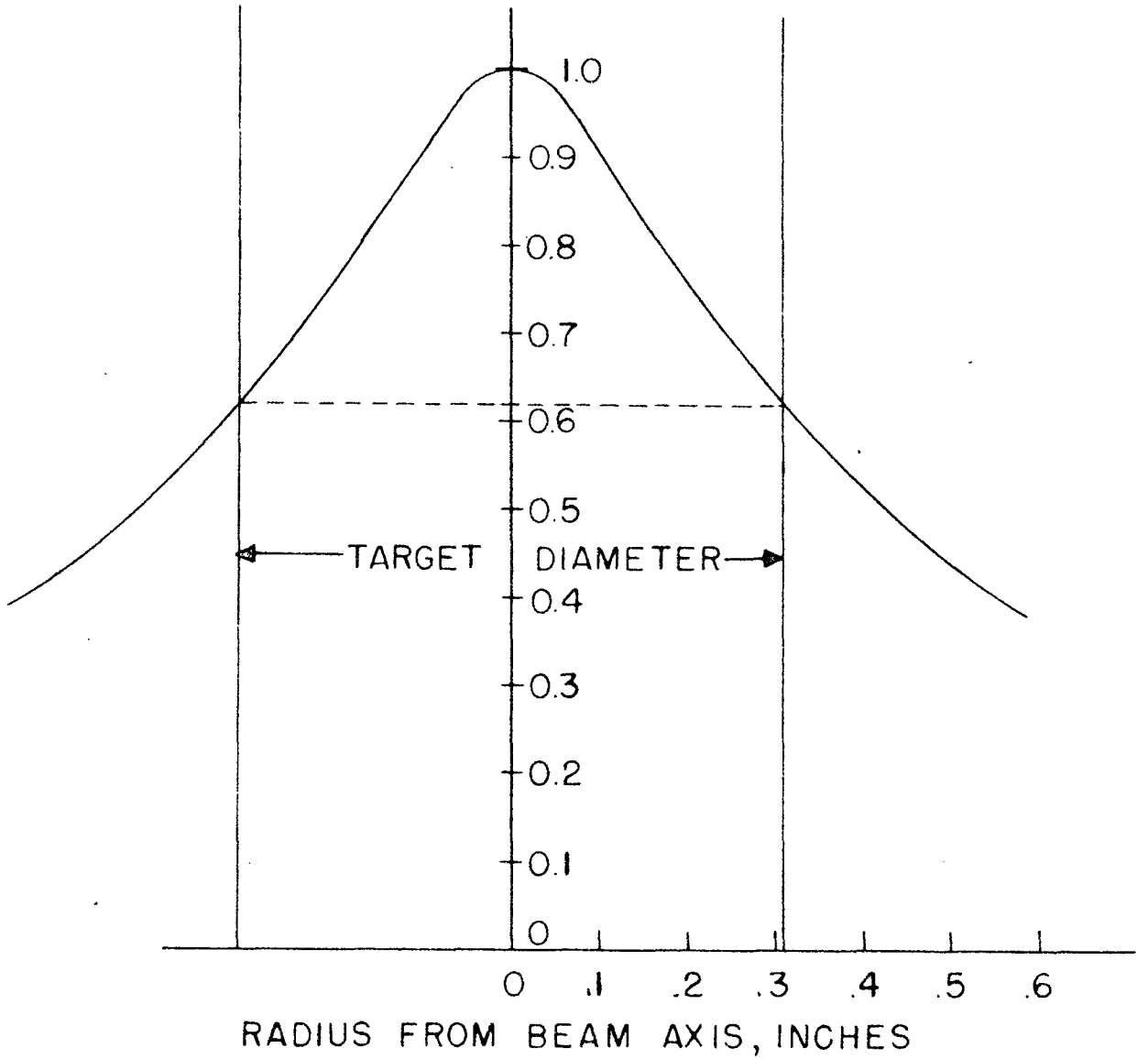

Fig. 8

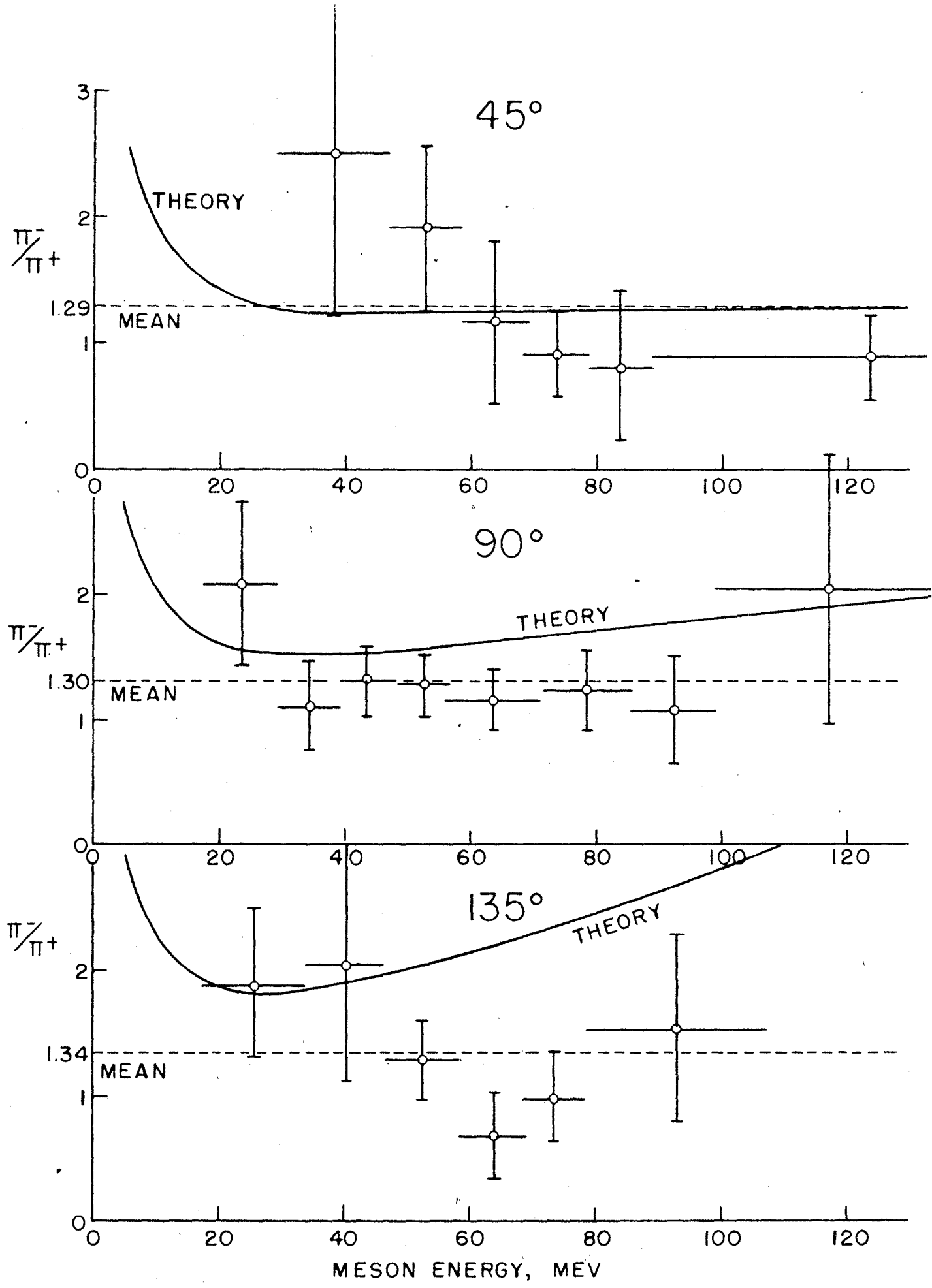
45°
THEORY
π^-/π^+
1.29
MEAN
90°
THEORY
π^-/π^+
1.30
MEAN
135°
THEORY
π^-/π^+
1.34
MEAN
0
1
2
3
0
20
40
60
80
100
120
MESON ENERGY, MEV

Fig. 9

14912-1

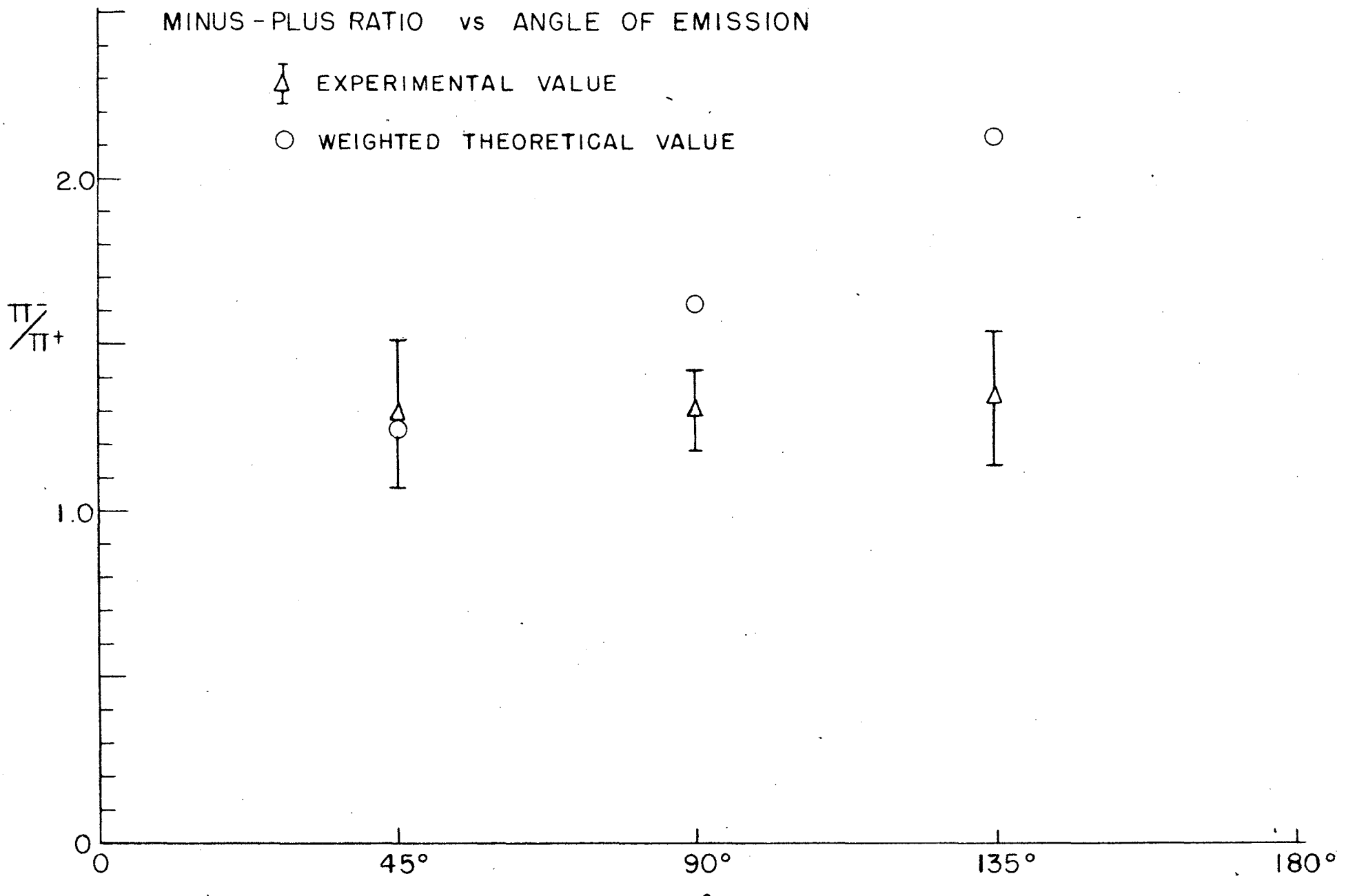

Fig. 10

14905-1

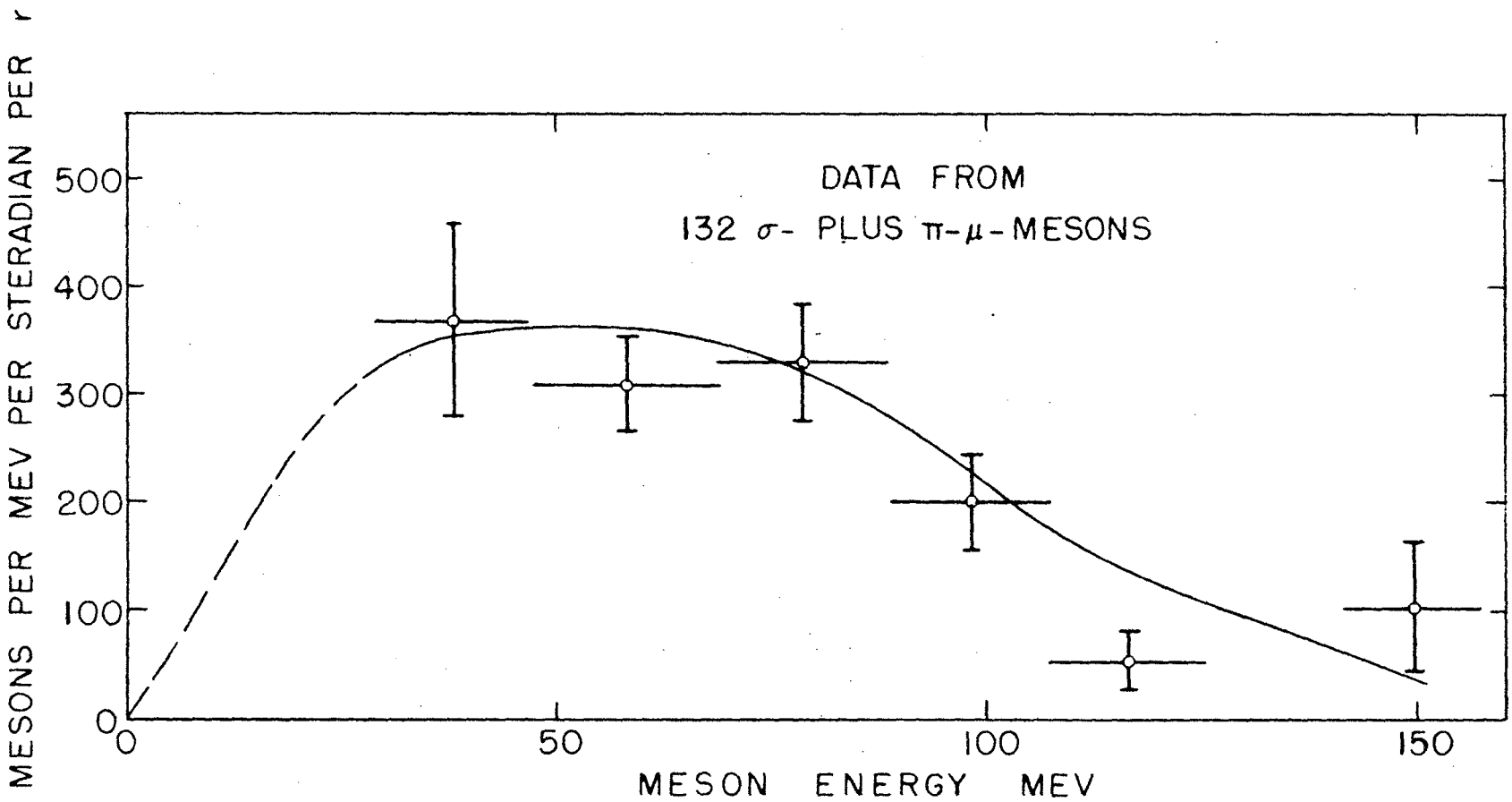

ENERGY SPECTRUM FROM CARBON AT 45°

Fig. 11

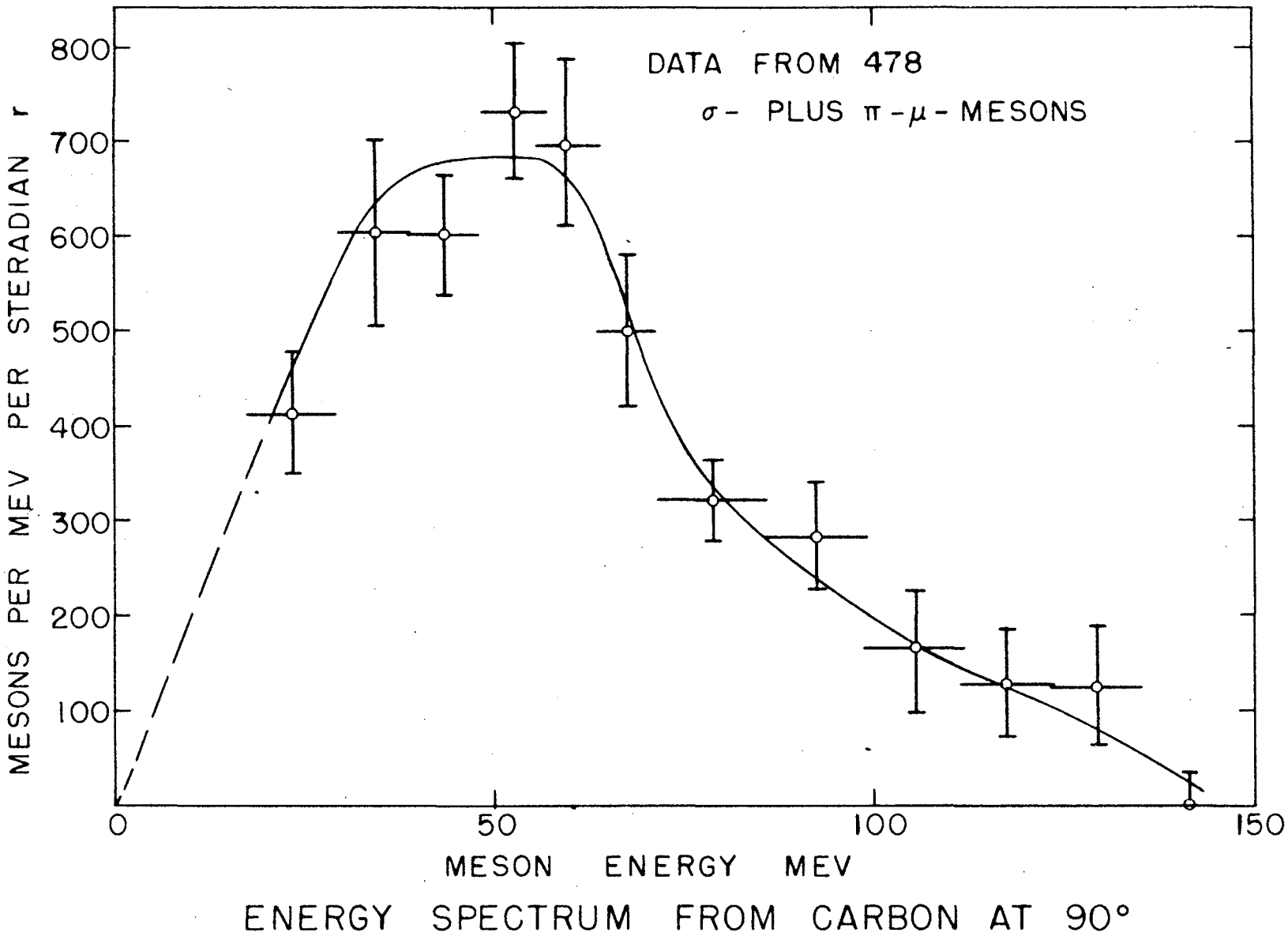

ENERGY SPECTRUM FROM CARBON AT 90°

Fig. 12

14951-1

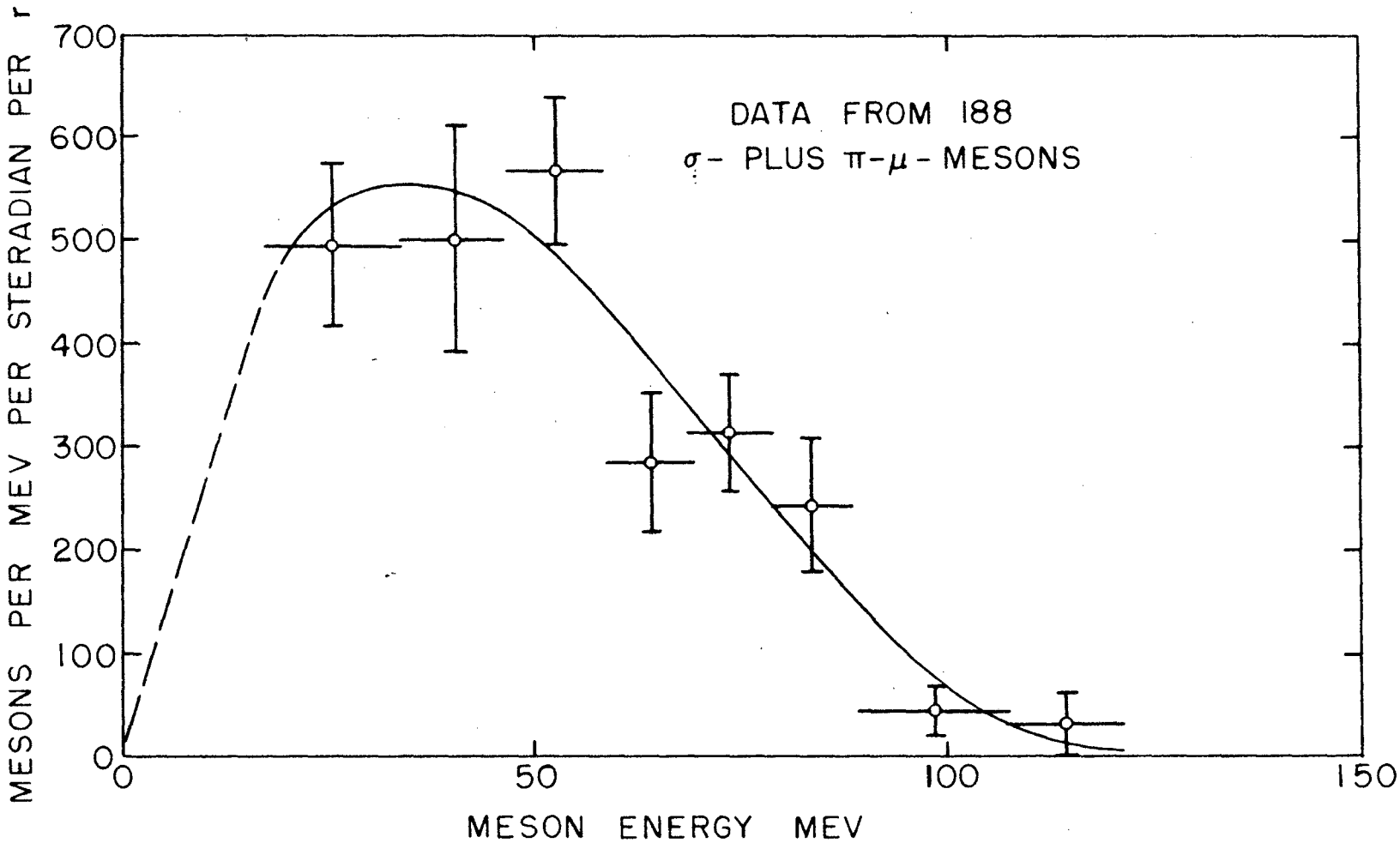

ENERGY SPECTRUM FROM CARBON AT 135°

Fig. 13

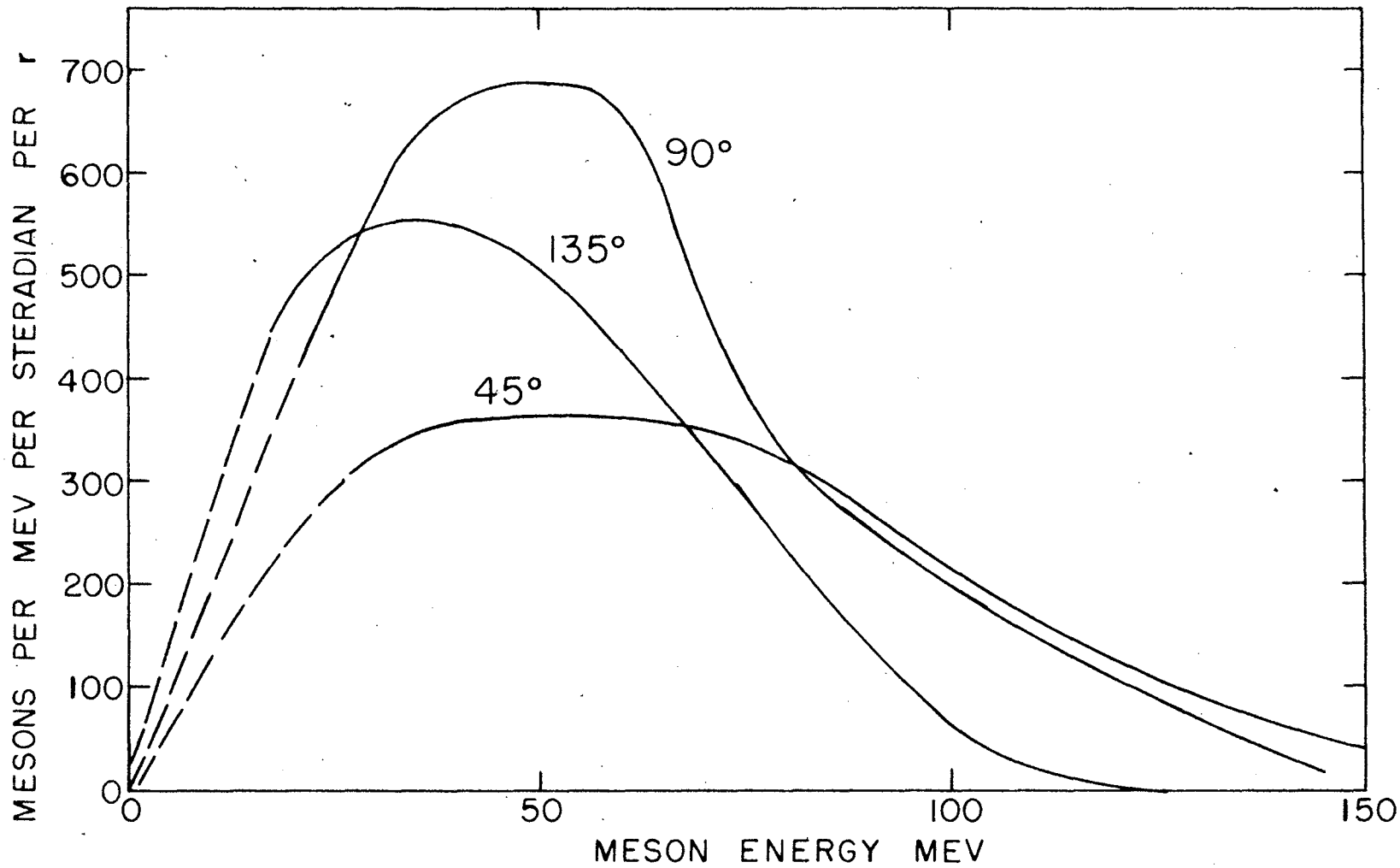

ENERGY SPECTRUM FROM CARBON FOR THREE ANGLES

Fig. 14

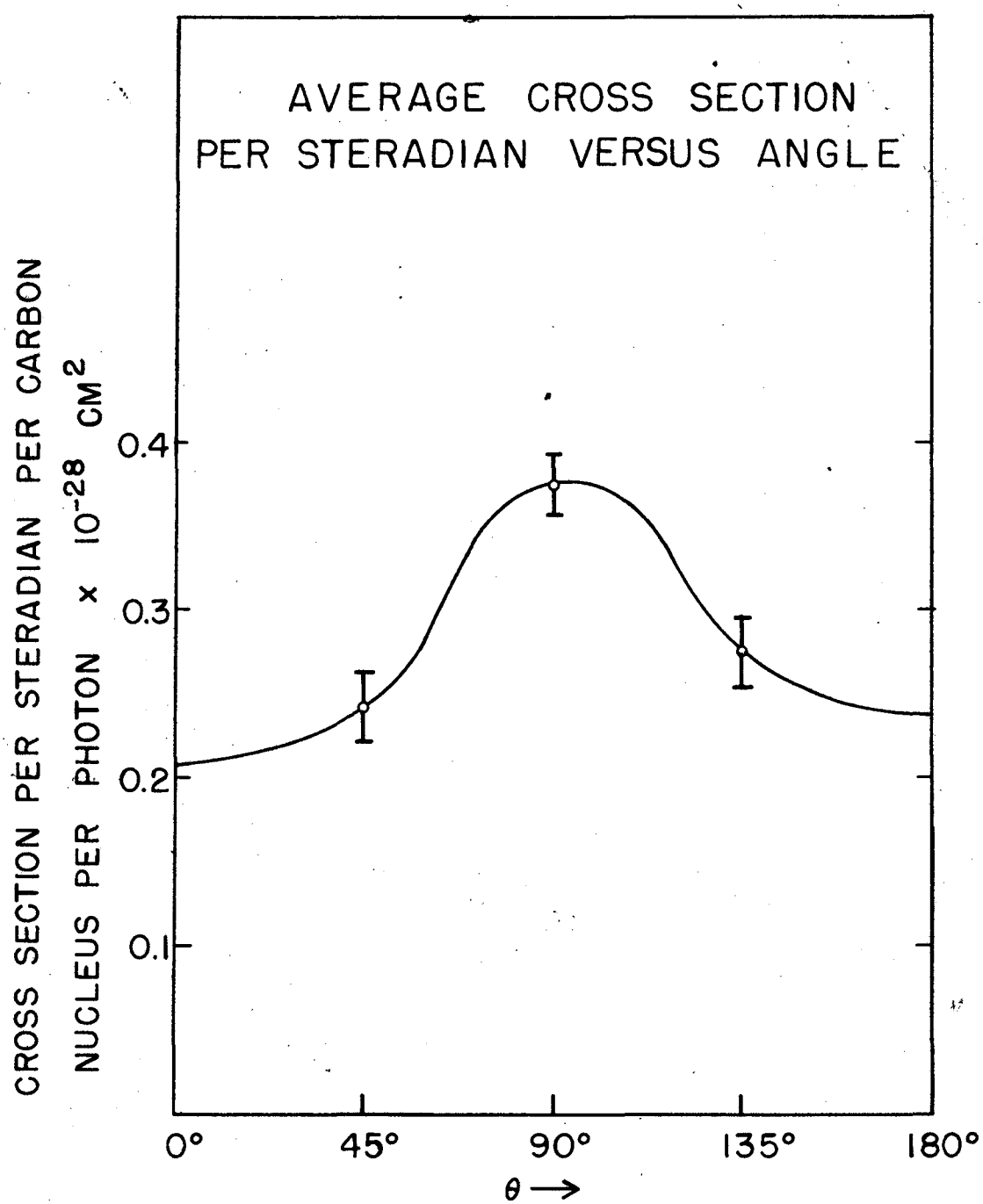
AVERAGE CROSS SECTION
PER STERADIAN VERSUS ANGLE
CROSS SECTION PER STERADIAN PER CARBON
NUCLEUS PER PHOTON x 10^{-28} CM^2
0.4
0.3
0.2
0.1
0°
45°
90°
135°
180°
θ →

Fig. 15

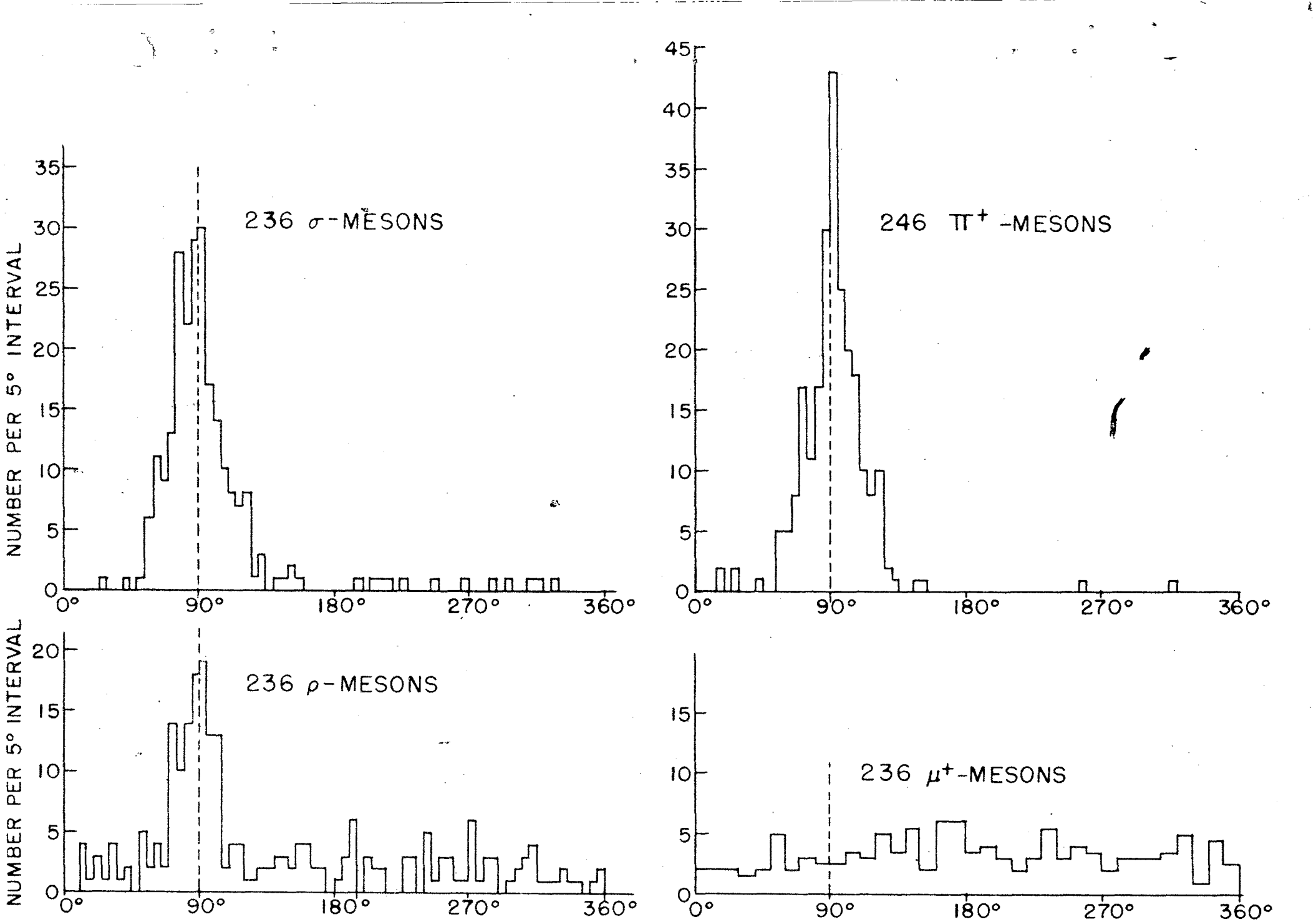

90° ANGULAR DISTRIBUTION

Fig. 16

14902-1

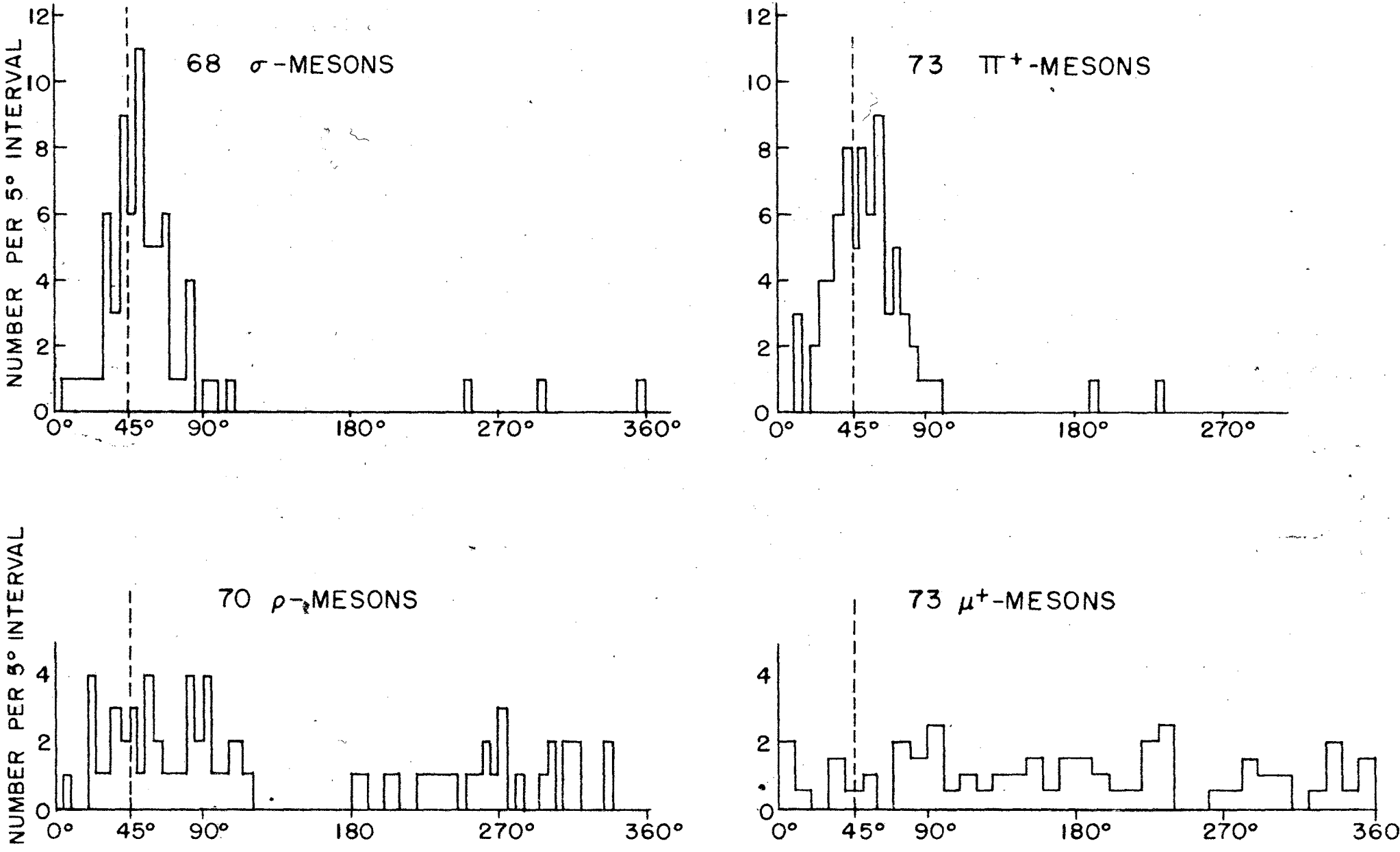

45° ANGULAR DISTRIBUTIONS

Fig. 18

14901-

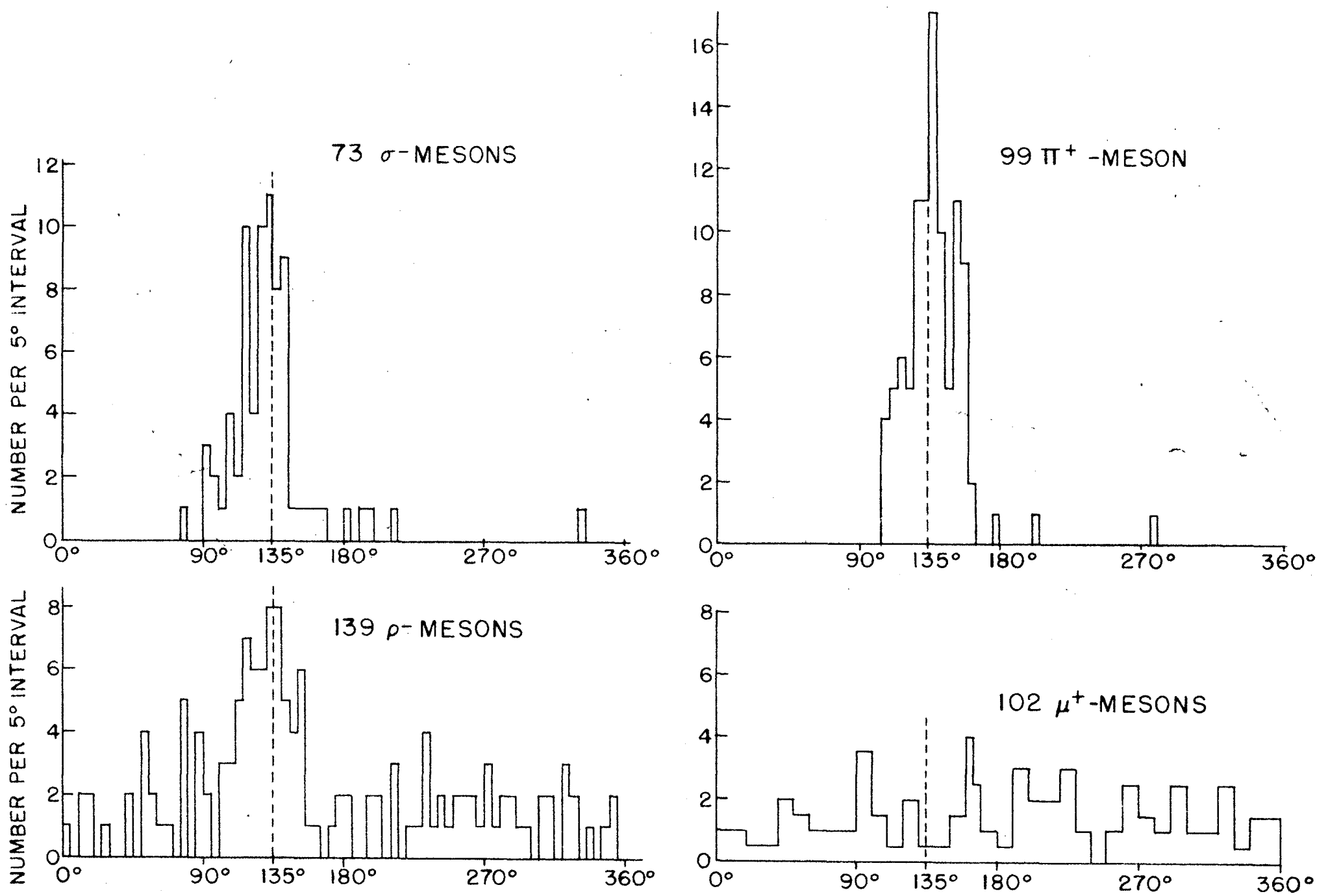

135° ANGULAR DISTRIBUTIONS

14903-1

Fig. 19